YOKOHAMA National University

Electrocatalyst of Alkaline Water Electrolysis for Fluctuated Operation and SPE Membrane Electrolysis for Energy Carrier Synthesis with Water Decomposition

Shigenori MITSUSHIMA

Green Hydrogen Research Center, Yokohama National University,

Institute of Advanced Sciences (IAS), Yokohama National University

2 Hydrogen production, and transportation

Alkaline Water electrolysis

- ✓ Start & stop impact for electrodes in a bipolar electrolyzer
- ✓ Design of (Li)NiO/Ni durable anode

$H_2O \rightarrow H_2 + 1/2O_2$ **U^o = 1.23 V**

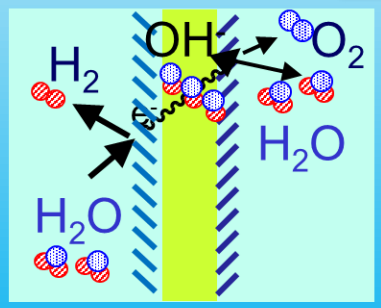

Electrohydrogenation of toluene with water decomposition

- ✓ Introduction of a new electrolyzer system using PEFC technology

$C_6H_5CH_3 + 3\,H_2O \rightarrow C_6H_{11}CH_3 + 3/2O_2$ **U^o = 1.08 V**

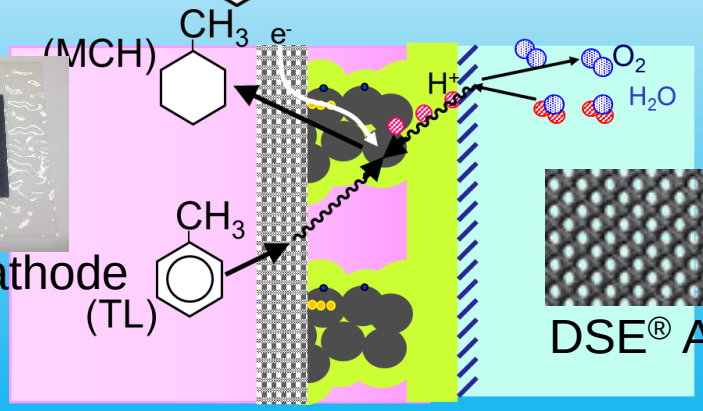

Electrode-cathode assembly

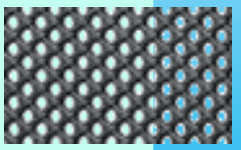

DSE® Anode

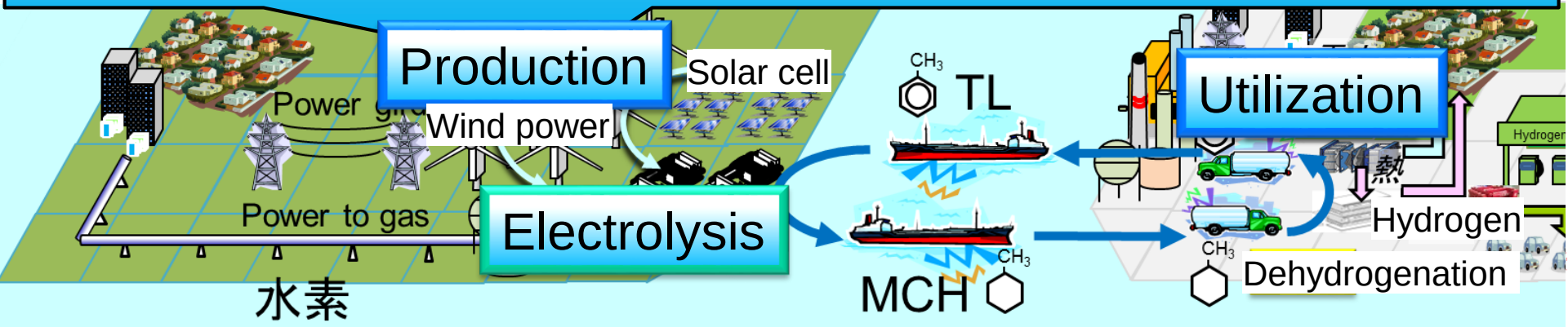

Contents

1. Introduction
2. Analysis of bipolar electrolyzer for alkaline water electrolysis
3. Active and durable anode for alkaline water electrolysis
4. Direct electrohydrogenation of toluene with water decomposition
5. Conclusion

4 C and H cycle in global energy system

Fossil fuels: natural extremely slow cycle
Biomass: natural annually or decadal cycle
Hydrogen: artificial carbon free cycle

Photosynthesis

Renewal electricity

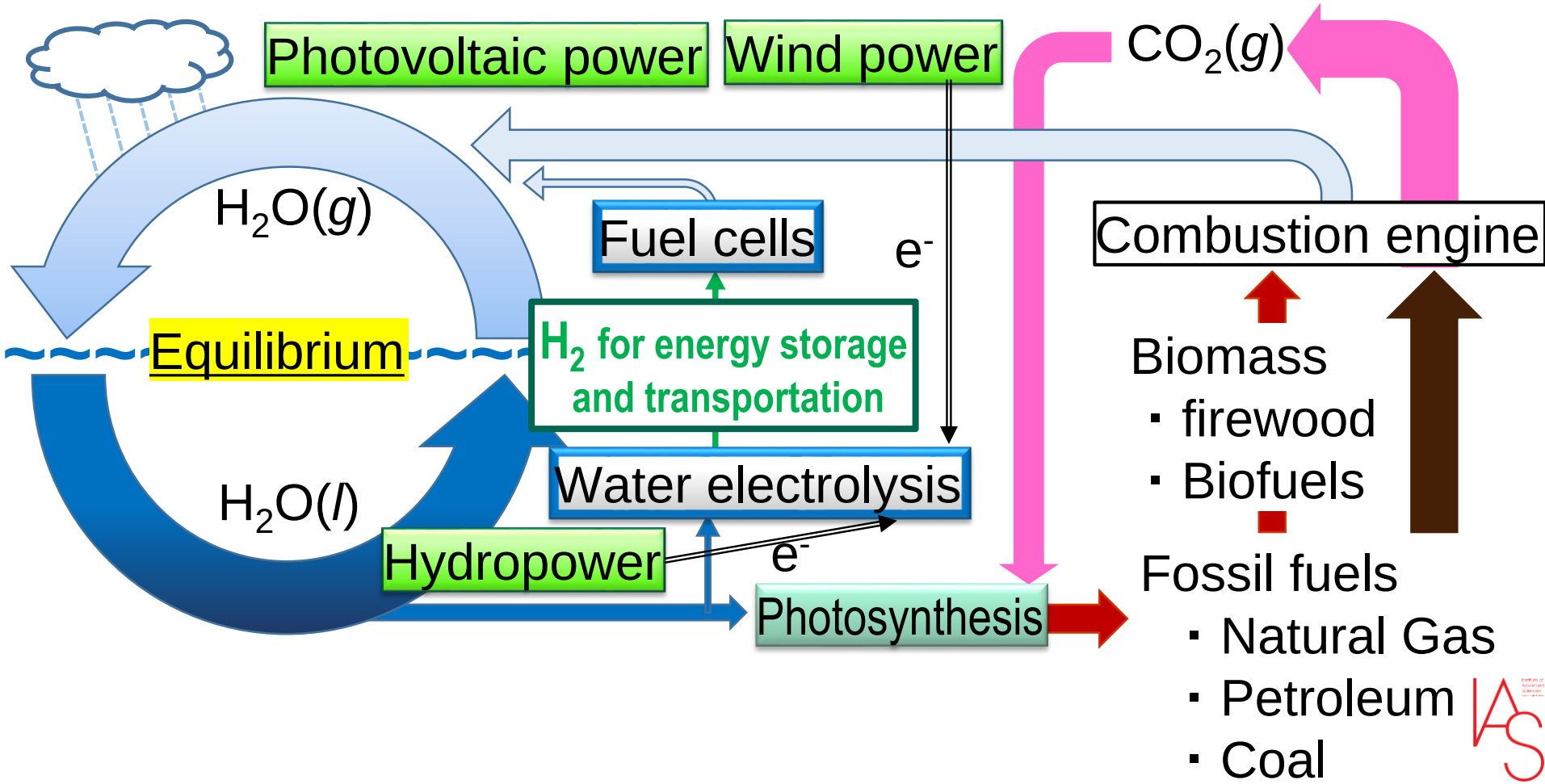

5 Role of hydrogen and water electrolysis

Water + Electricity → Water electrolyzer → Hydrogen

- Conversion of electricity to chemical energy
  - Usage of excess renewable electricity to meet demand = Power supply following operation with start & stop operation

    Less expensive, compact & durable

- Storage electricity as chemical energy
  - Usage as energy carrier, but low volumetric energy density is a issue for long term storage and oversea transportation

    Liquidification (L-H_2, L-NH_3, or Organic chemical hydride)

Performance of AWE and SPEWE

SPEWE has higher density for H_2 production than AWE
Both system should be designed around 1.8 ~ 2.0 V of cell voltage

||
Almost same OPEX

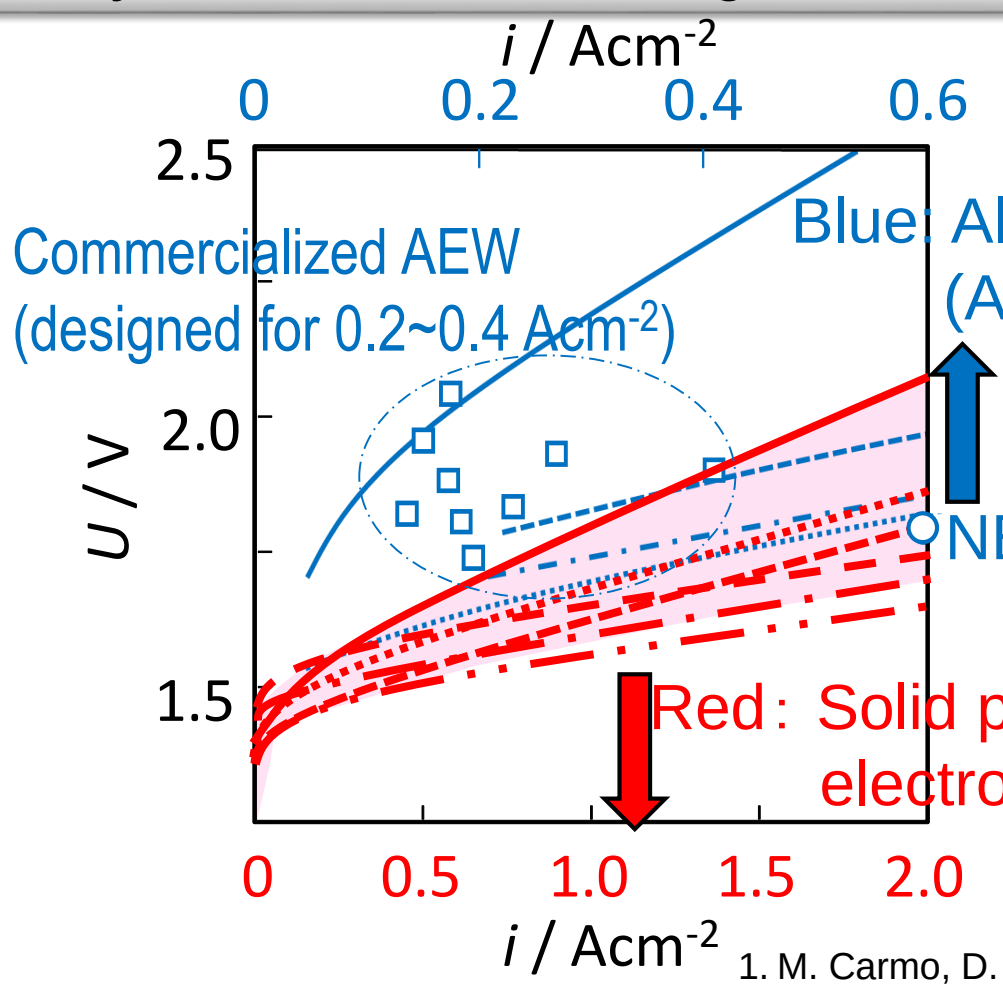

Blue: Alkaline water electrolysis (AWE)

○NEDO project of '17

Red: Solid polymer electrolyte water electrolysis (SPEWE)

1. M. Carmo, D. L. Fritz, J. Mergel, and D. Stolten, Int. J. Hydrogen Energy **38**, 4901 (2013).
2. S. Mitsushima, S. Fujita, ELECTROCHEMISTRY **85**, 28 (2017).

7 Type of water electrolysis and its characteristics

	Basic electrolyte	Acidic electrolyte
Solid polymer electrolyte (Ion exchange membrane)	~1 A cm^{-2} @1.8 V PGM → NPGM catalyst ✓ Instable & low conductive electrolyte membrane ⇒ reverse current if electrolyte feed	2 – 3 A cm^{-2} @1.8 V PGM catalyst Ti base materials ✓ High material cost ✓ Pure water feed SPEWE
Diaphragm (Porous membrane)	0.2 – 0.6 A cm^{-2} @1.8 V NPGM catalyst Stainless based materials ✓ Low current density ✓ KOH solution feed ⇒reverse current AWE	

Today's talk

Basic electrolyte

- Understanding of reverse current
- Development of durable electrocatalyst

Acidic electrolyte with SPE

- Value added water electrolysis: direct energy carrier synthesis

Contents

1. Introduction
2. Analysis of bipolar electrolyzer for alkaline water electrolysis
3. Active and durable anode for alkaline water electrolysis
4. Direct electrohydrogenation of toluene with water decomposition
5. Conclusion

9 Reverse current for bipolar electrolyzer

After shut down operation: $U \approx 1.3 \rightarrow 0.3$ V

Anode: $NiOOH + H2O + e^- \rightarrow Ni(OH)_2 + OH^-$ (reduction)

Cathode: $Ni + 2OH^- \rightarrow Ni(OH)_2 + 2e^-$ (oxidation)

Degradation

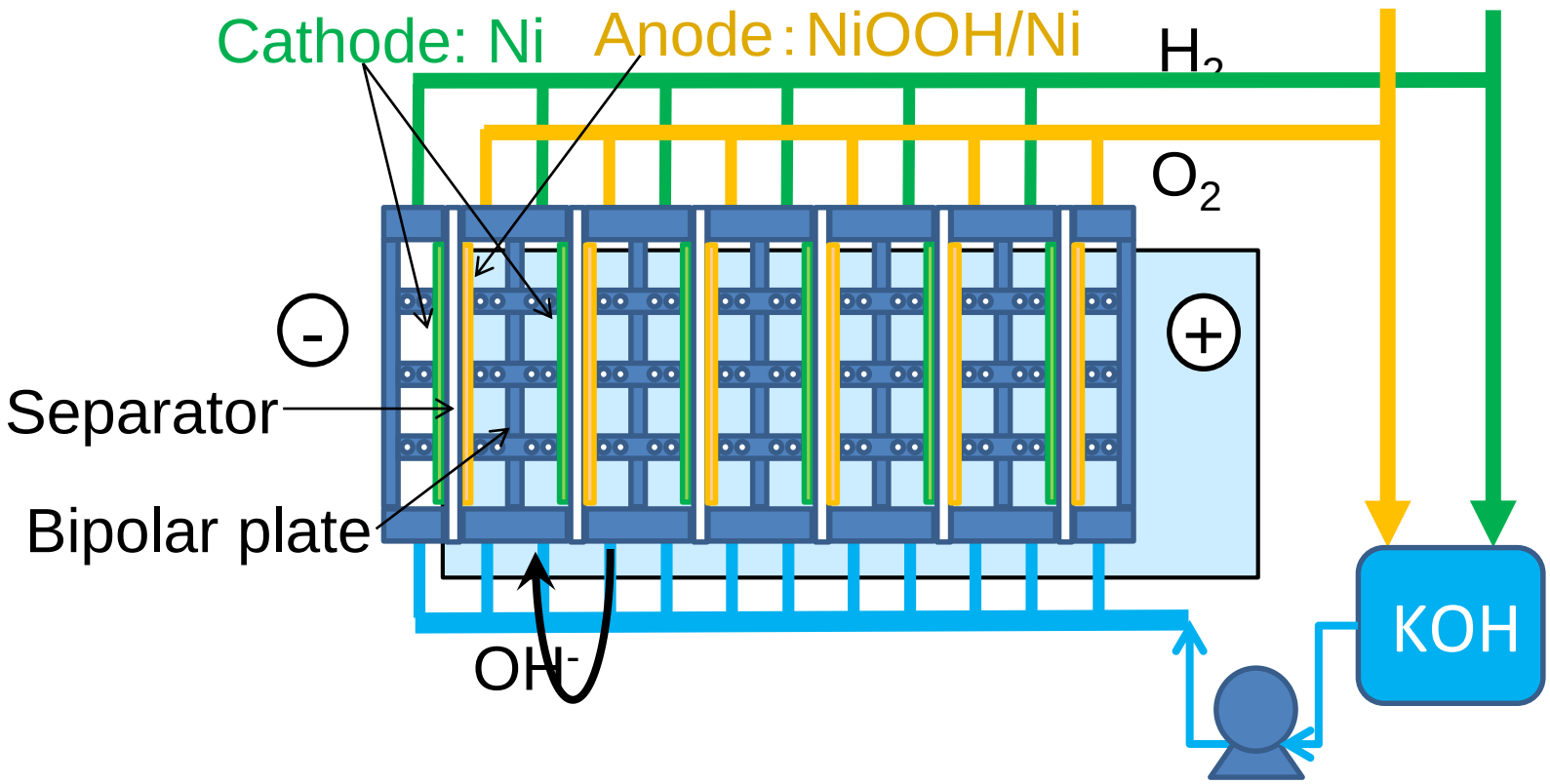

Y. Uchino, T. Kobayashi, S. Hasegawa, I. Nagashima, Y. Sunada, A. Manabe, Y. Nishiki, S. Mitsushima, Electrocatalysis. (2017). doi:10.1007/s12678-017-0423-5.

10 Measurement system of leak & reverse current

Leak and reverse current was measured as ionic current through manifolds using clamp meter

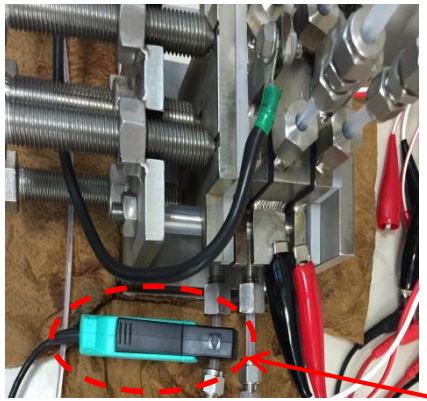

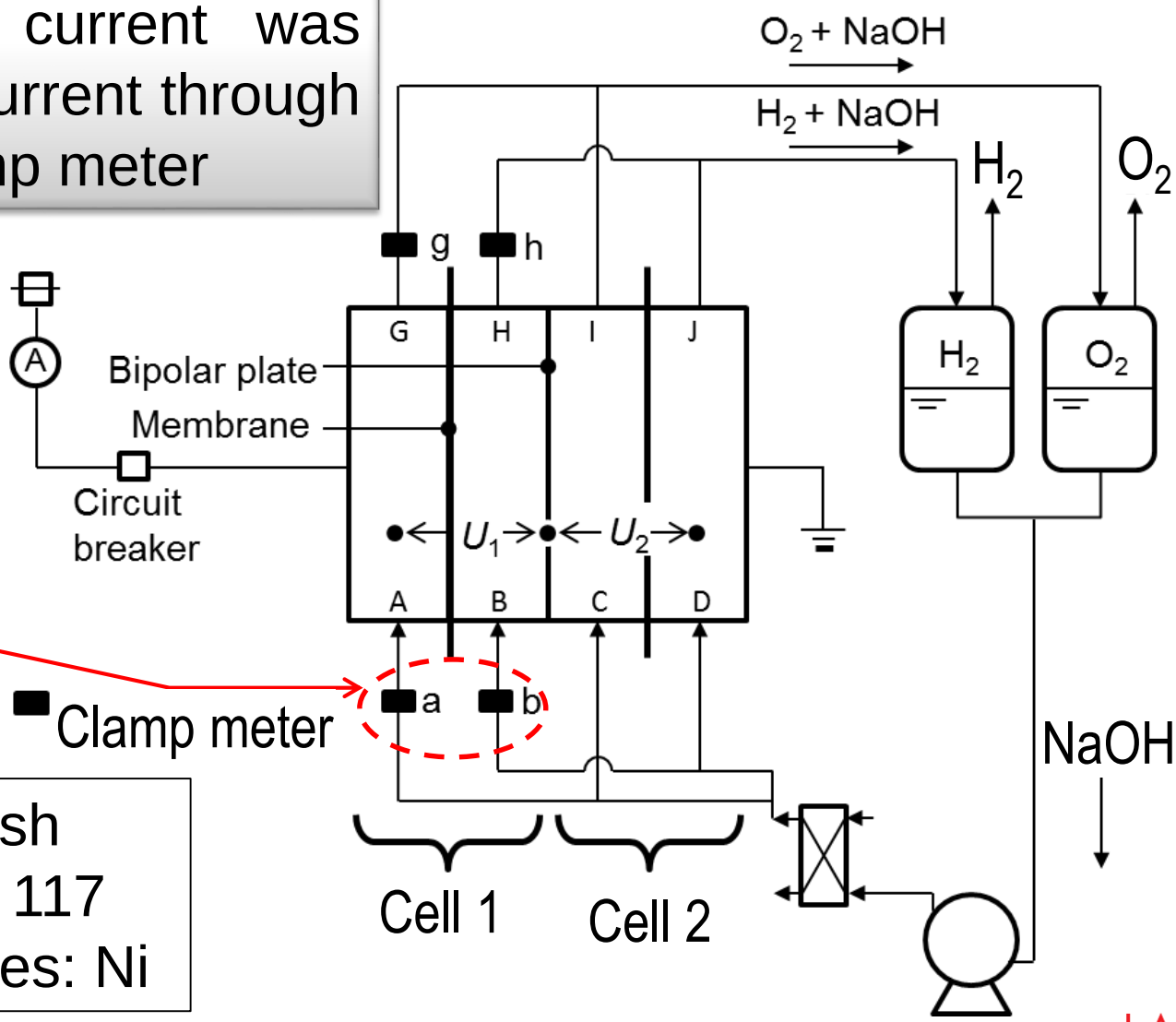

- Electrodes: Ni mesh
- Separator: Nafion 117
- End & bipolar plates: Ni

Y. Uchino, T. Kobayashi, S. Hasegawa, I. Nagashima, Y. Sunada, A. Manabe, Y. Nishiki, S. Mitsushima, Electrocatalysis. (2017). doi:10.1007/s12678-017-0423-5.

11 Equivalent circuit & performance of the electrolyzer

- Cell performances in a electrolyzer were almost the same
- Reverse current was determined as a function of the condition of electrolysis to analyze potential change of electrodes after electrolysis

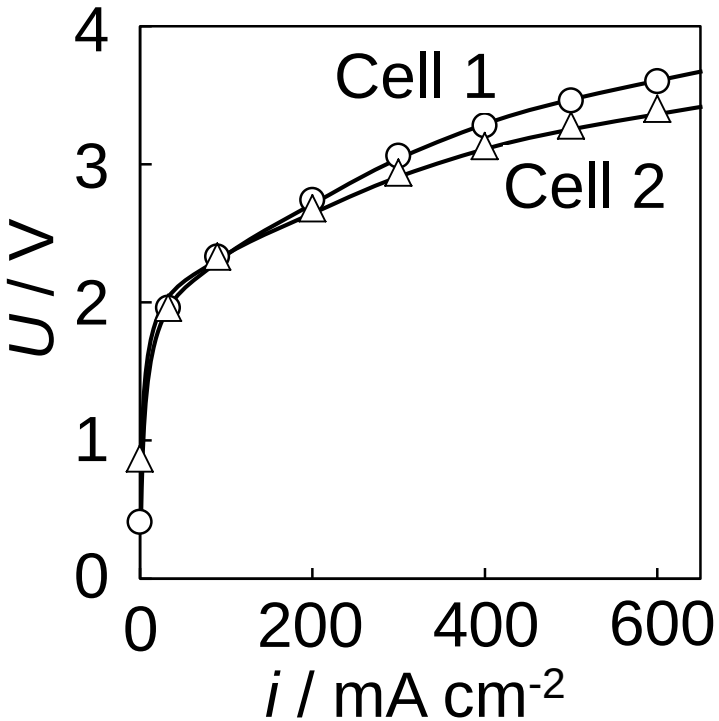

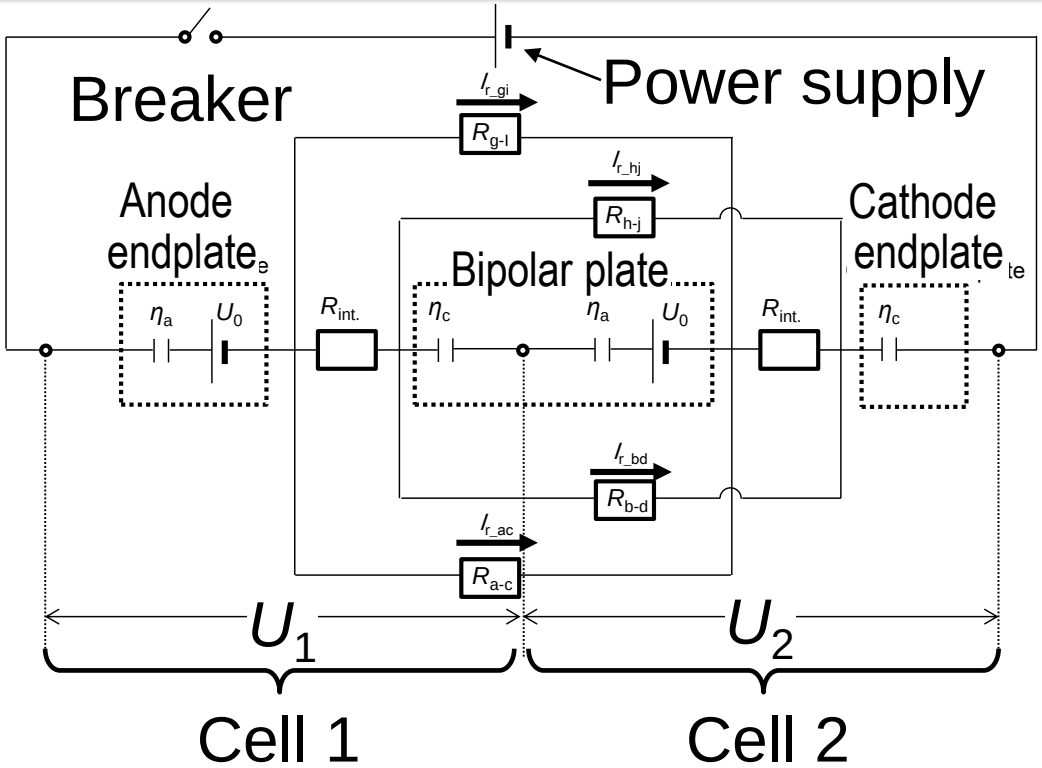

Y. Uchino, T. Kobayashi, S. Hasegawa, I. Nagashima, Y. Sunada, A. Manabe, Y. Nishiki, S. Mitsushima, Electrocatalysis. (2017). doi:10.1007/s12678-017-0423-5.

12 Reverse current and cell voltage as a function of time

- U_1 and U_2 decreased slightly and significantly, respectively
- This behavior could be explained with discharge of the bipolar plate

Reverse current is a function of cell voltage and ionic resistances

$$I_r = 4\,\{U_2 - (U_{1_initial} - U_1)\} / (R_{manifold} + R_{internal})$$

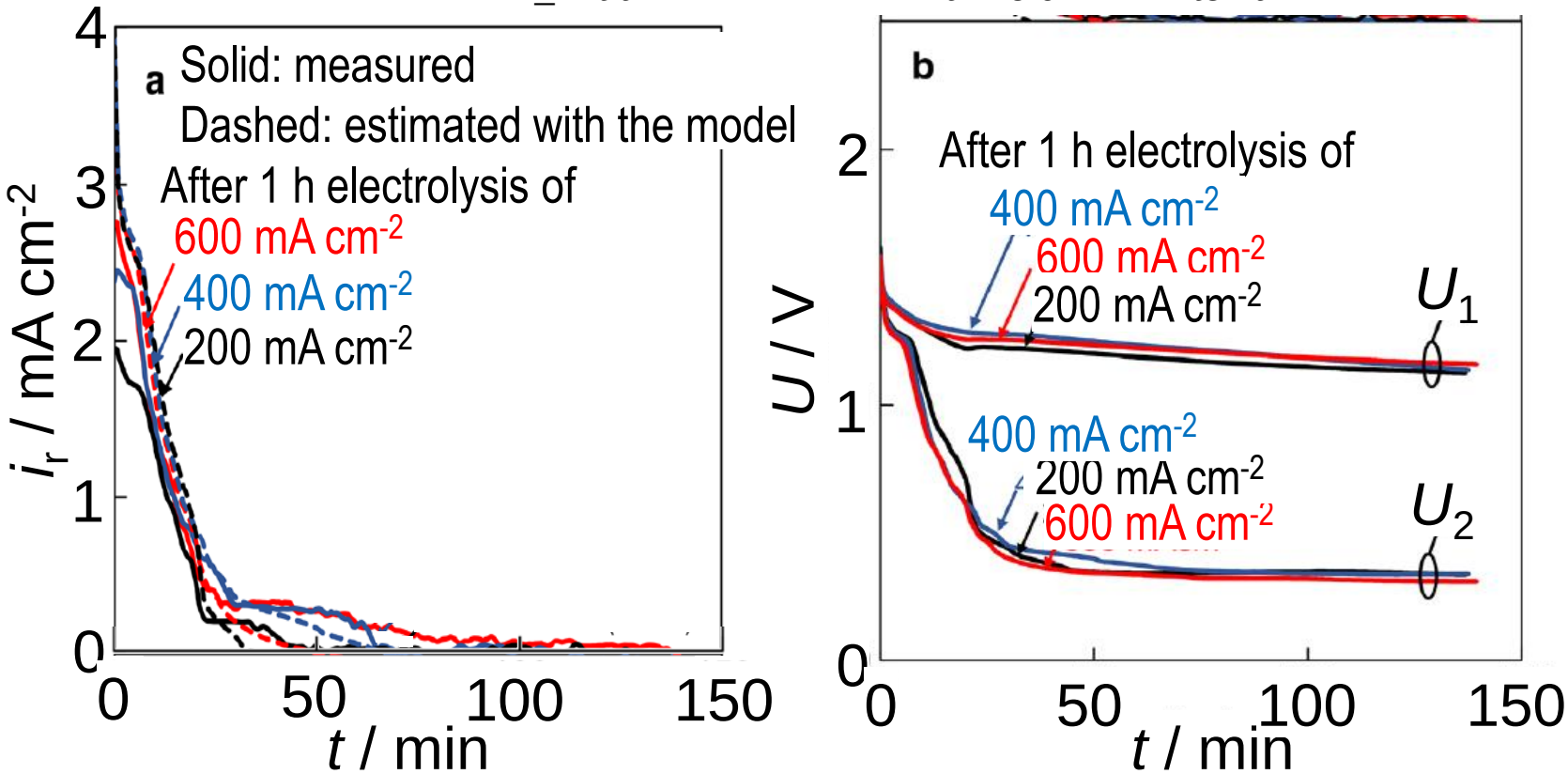

Y. Uchino, T. Kobayashi, S. Hasegawa, I. Nagashima, Y. Sunada, A. Manabe, Y. Nishiki, S. Mitsushima, Electrocatalysis. (2017). doi:10.1007/s12678-017-0423-5.

13 Electric charge of reverse current

Charge of reverse current increased with current density of electrolysis = *Q* was almost proportional to NiOOH formation

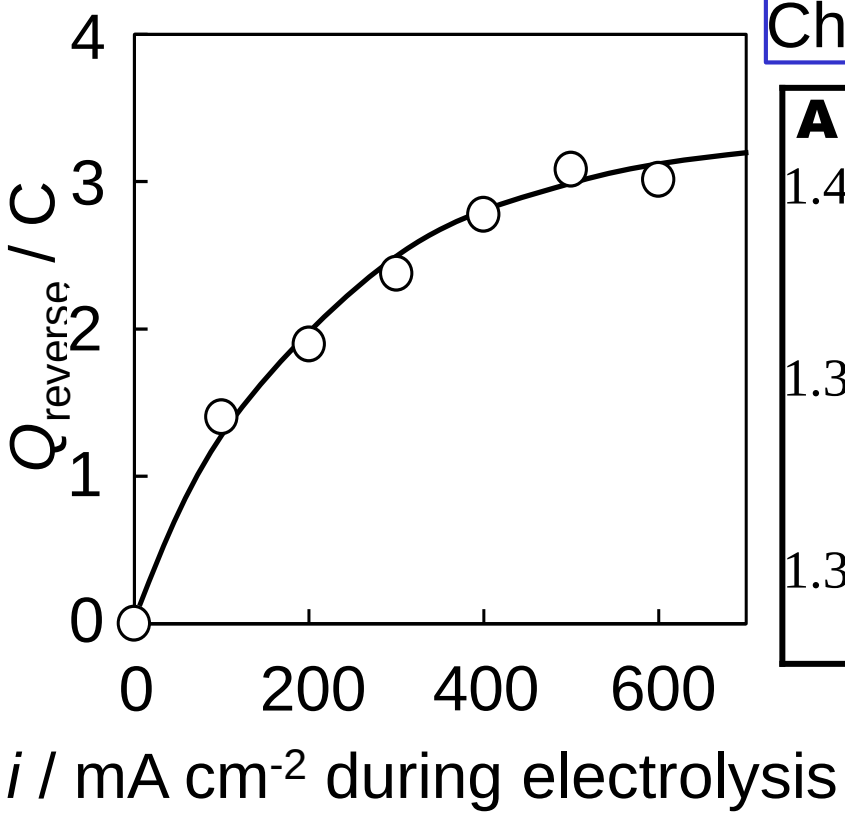

Change of surface with reverse current

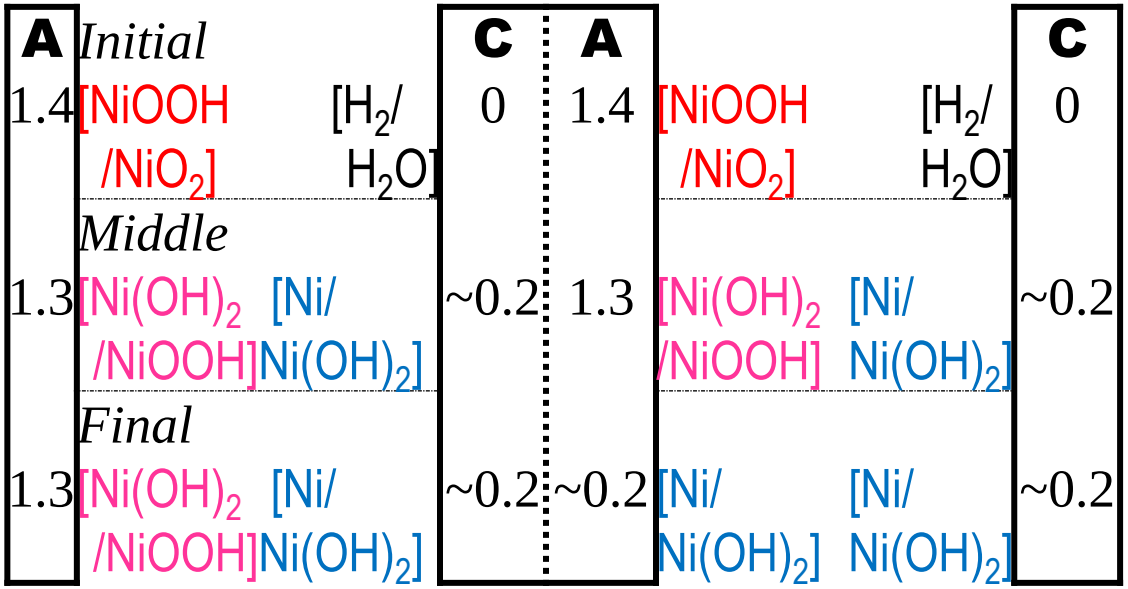

Y. Uchino, T. Kobayashi, S. Hasegawa, I. Nagashima, Y. Sunada, A. Manabe, Y. Nishiki, S. Mitsushima, Electrocatalysis. (2017). doi:10.1007/s12678-017-0423-5.

14 Conclusion for start & stop of AWE

The reverse current in alkaline water electrolyzer having relation between the electrolyzer operating conditions and cell voltage has been investigated using a bipolar-type electrolyzer which consists of two cells.

- ✓ The reverse current increased with the current density of the electrolysis.
- ✓ The increase in the charge of the reverse current would correspond to the increase of the surface oxide on the anode of the bipolar plate.
- ✓ Cell voltages were above 1.4 V at all cases just when the electrolyzer is opened the circuit to stop. Therefore, the major redox couple of the reverse current would be [NiOOH/NiO_2 and [H_2/H_2O].
- ✓ **Final surface of bipolar plate is 0.11 to 0.44 V vs. RHE of [Ni/Ni$(OH)_2$] for both sides**

Contents

1. Introduction

2. Analysis of bipolar electrolyzer for alkaline water electrolysis

3. Active and durable anode for alkaline water electrolysis

4. Direct electrohydrogenation of toluene with water decomposition

5. Conclusion

16 Degradation of Ni under 1.0~1.8 V(1 Vs^{-1}) of potential cycling

- OER current decreased with potential cycling
- Redox charge for Ni(II)/Ni(III) increased and its potential decreased with potential cycling
- OER current decreased a lot with formation of Ni(IV)

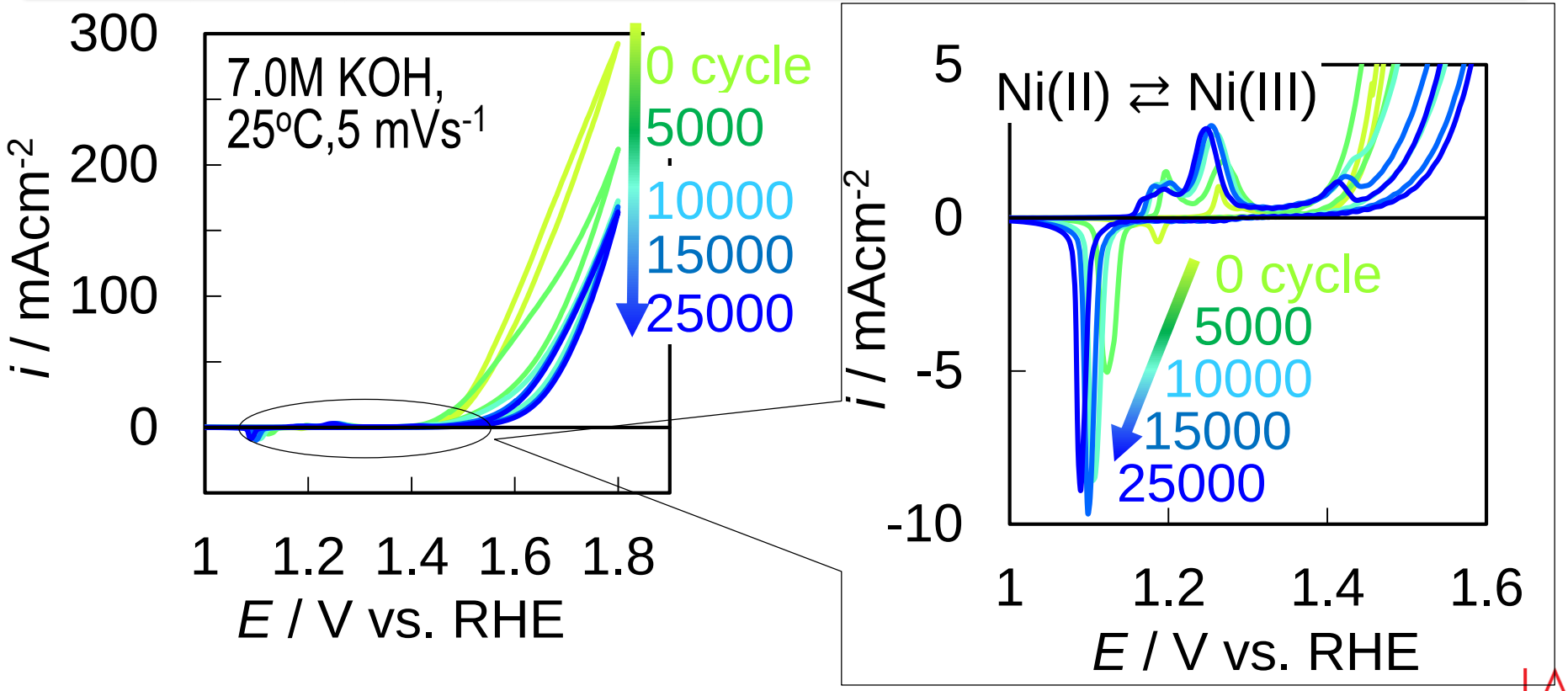

H. Ichikawa, K. Matsuzawa, Y. Kohna, I. Nagashimb, Y. Sunadc, Y. Nishikd, A. Manabd, and S. Mitsushima, *ECS Trans.*, 58 (2014) 9-15.

17 Idea of anode stabilization for AWE

- Active site is hydrous oxide
- In order to stabilize the hydrous layer, compact oxide layer must be stabilized = electronic conductive oxide layer that is synthesized at high temperature

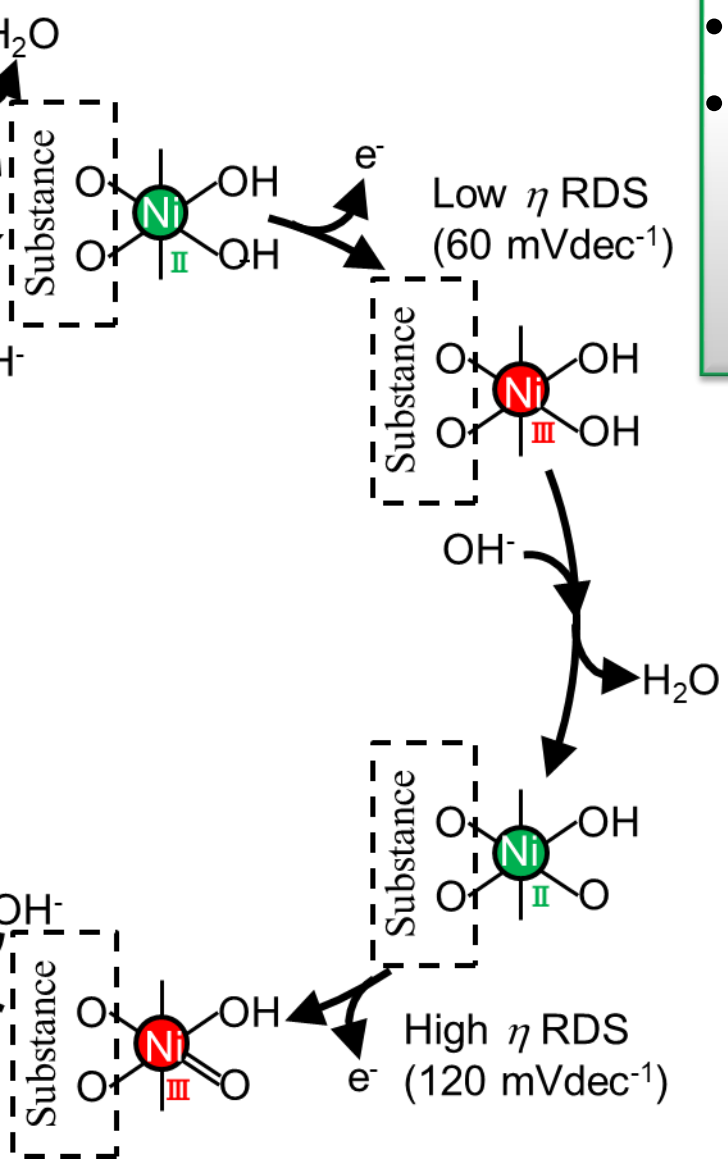

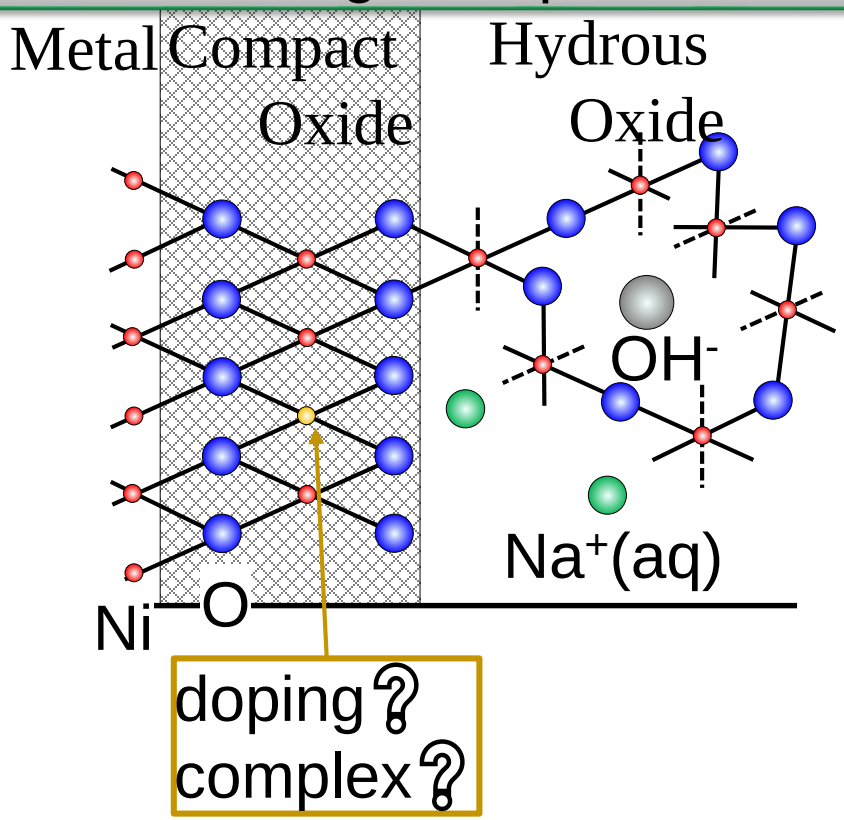

Illustration: based M. Lyons, R. Doyle, I. Godwin, M. O'Brien, L. Russell, *J. Electrochem. Soc.*, **159**, H932(2012)

18 Preparation of the Li dope NiO coated Ni

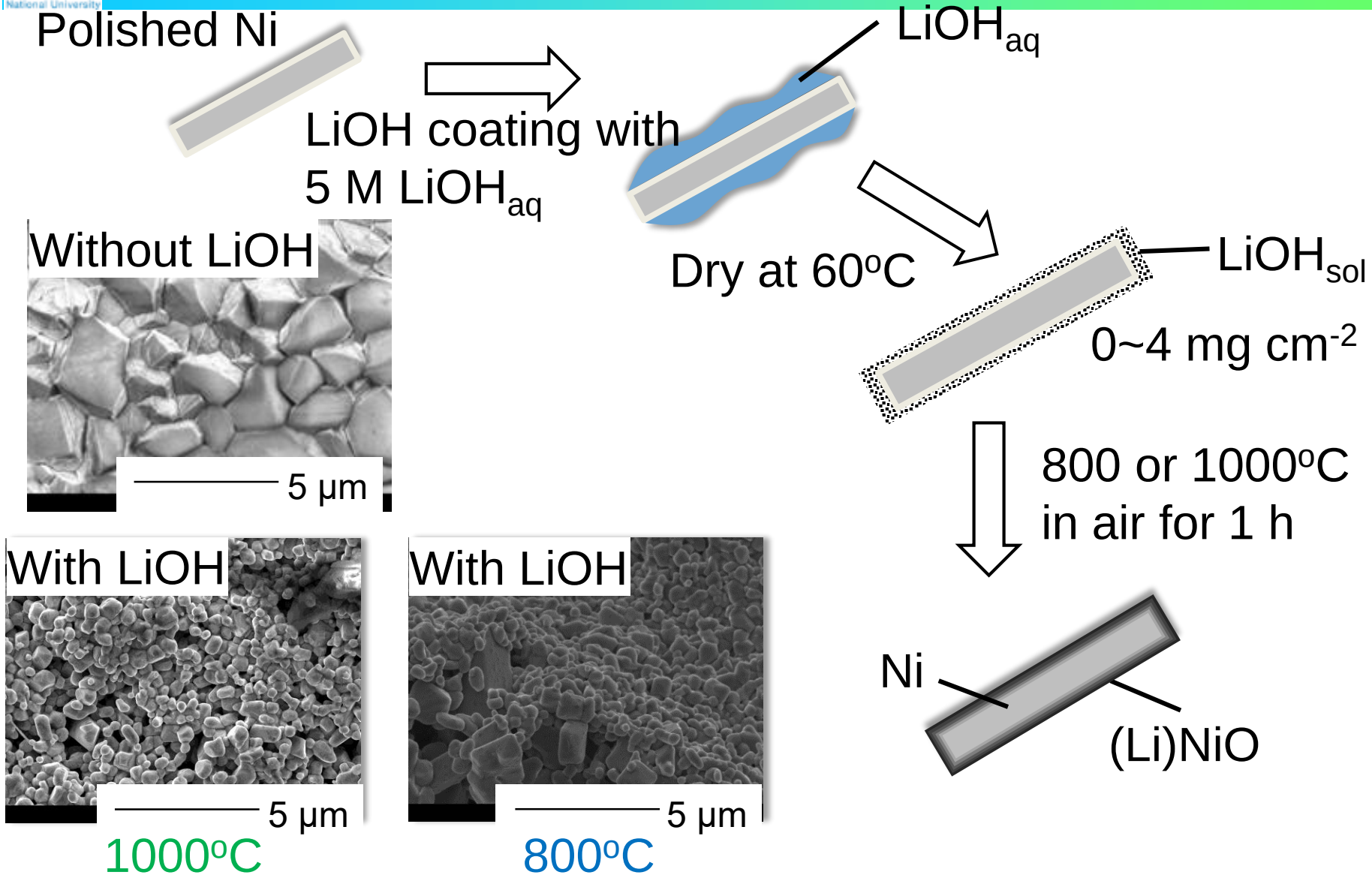

S. Fujita, I. Nagashima, Y. Sunada, Y. Nishiki, S. Mitsushima, Electrocatalysis. 8 (2017) 422–429.

19 Resistance measurement for the surface oxide

- 2-probe AC impedance was applied
- Resistance was evaluated as high frequency side of intercept to real axis
- High concentration $NaCl_{aq}$ was impregnated to decrease contact resistance

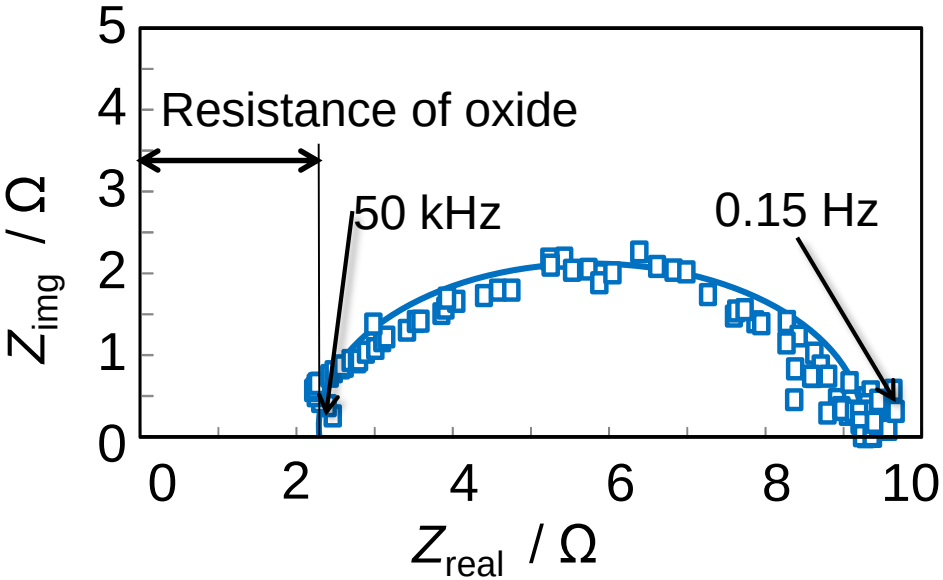

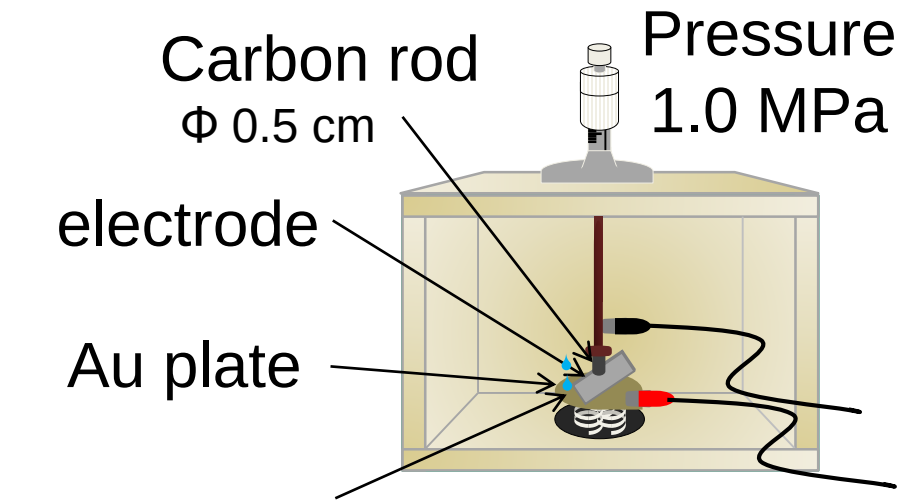

7.0 M $NaCl_{aq}$ was impregnated at the contact

S. Fujita, I. Nagashima, Y. Sunada, Y. Nishiki, S. Mitsushima, Electrocatalysis. 8 (2017) 422–429.

20 Electrochemical measurements

<Activity evaluation>

Slow scan voltammometry (SSV)

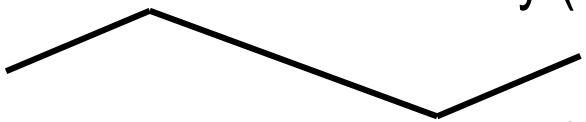

0.7 V - 1.8 V, 5 mV s^{-1}

<Degradation protocol>

Cyclic voltammometry (CV)

1.0 V - 1.8 V, 1 V s^{-1}

iR correction: AC impedance

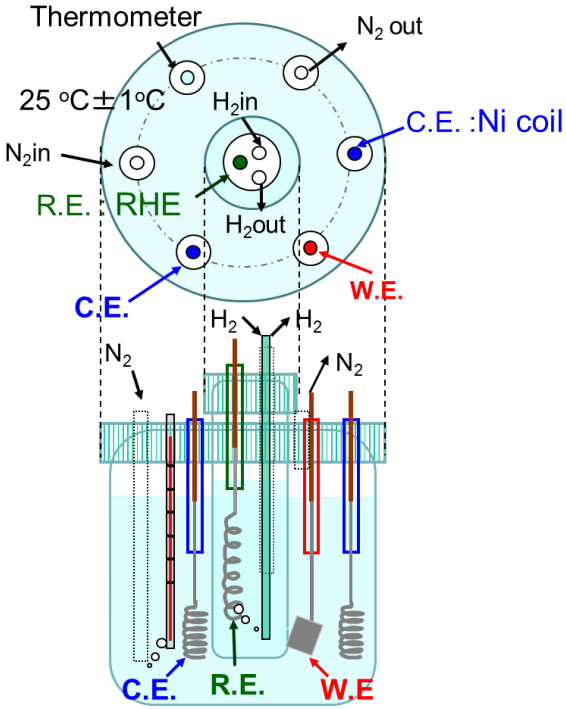

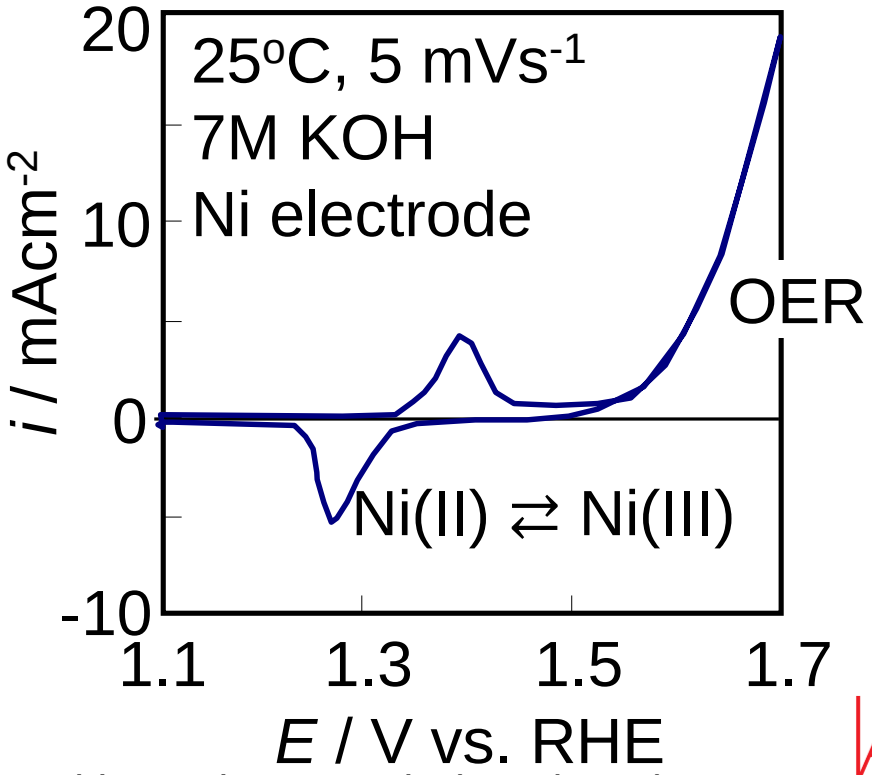

S. Fujita, I. Nagashima, Y. Sunada, Y. Nishiki, S. Mitsushima, Electrocatalysis. 8 (2017) 422–429.

21 XRD analysis for the surface oxide

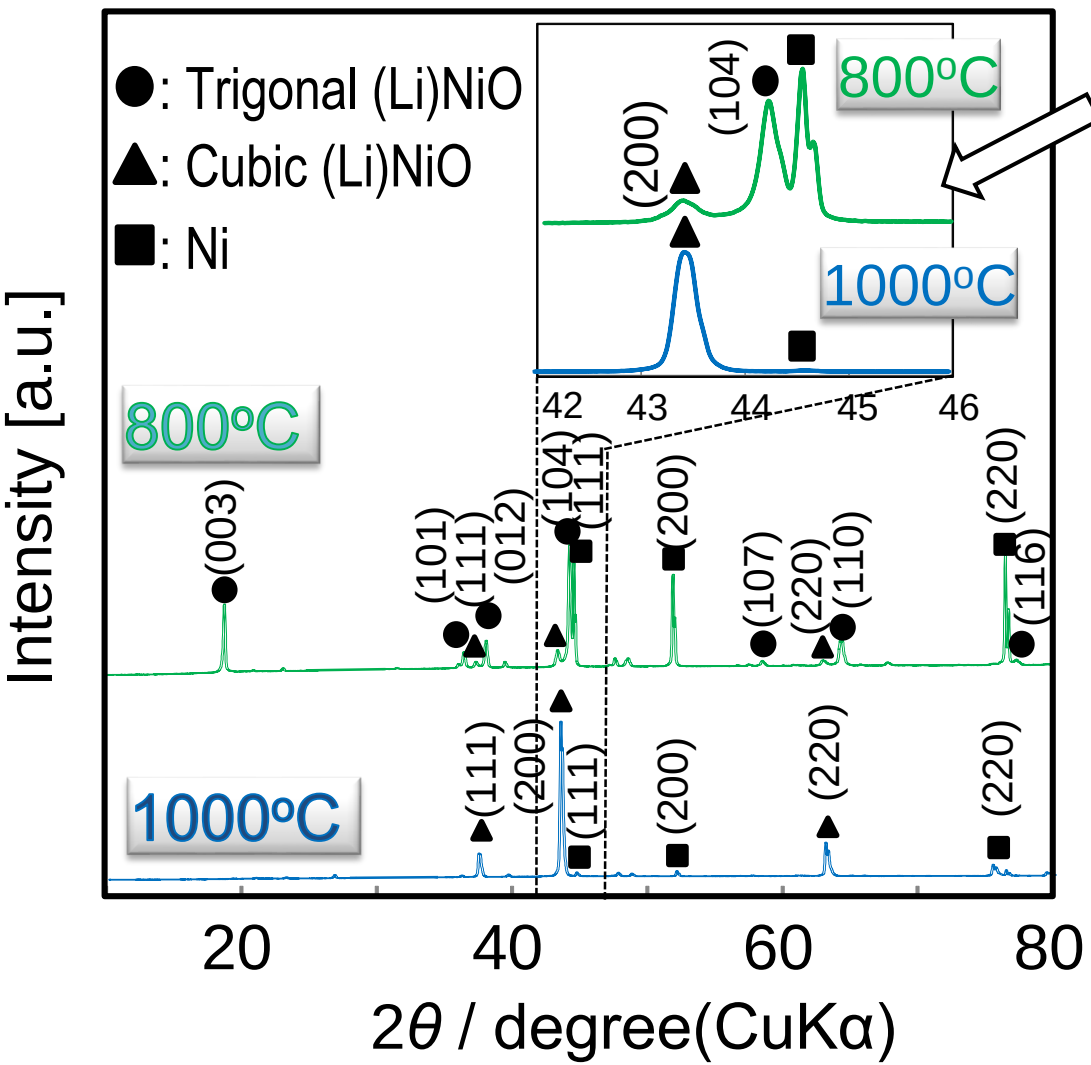

Peaks of (Li)NiO shifts higher angle with Li dopeing[4)] (Trigonal > Cubic)

800°C

- Thin oxide because of the existence of Ni peak
- Multi phases with trigonal and cubic

1000°C

- Single phase of cubic

S. Fujita, I. Nagashima, Y. Sunada, Y. Nishiki, S. Mitsushima, Electrocatalysis. 8 (2017) 422–429.

22 Relationship between resistance of oxide and composition

- Resistance of the oxide decreased with increase of the *x*
- For 800°C, high resistance cubic phase affected the oxide resistance

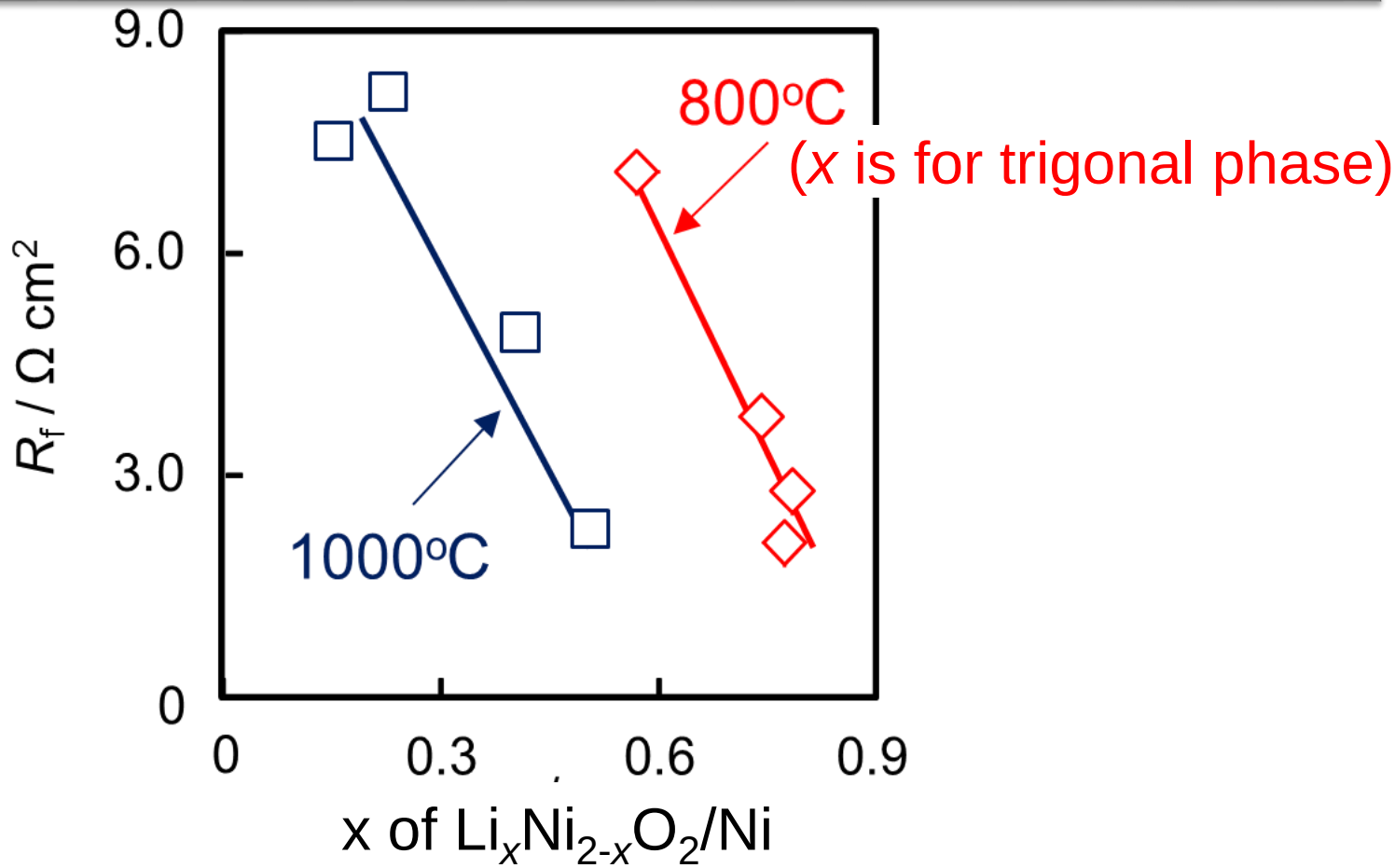

S. Fujita, I. Nagashima, Y. Sunada, Y. Nishiki, S. Mitsushima, Electrocatalysis. 8 (2017) 422–429.

Performance as a function of Li dope amount

Li dope amount optimum would be balance of catalytic activity and electronic conductivity

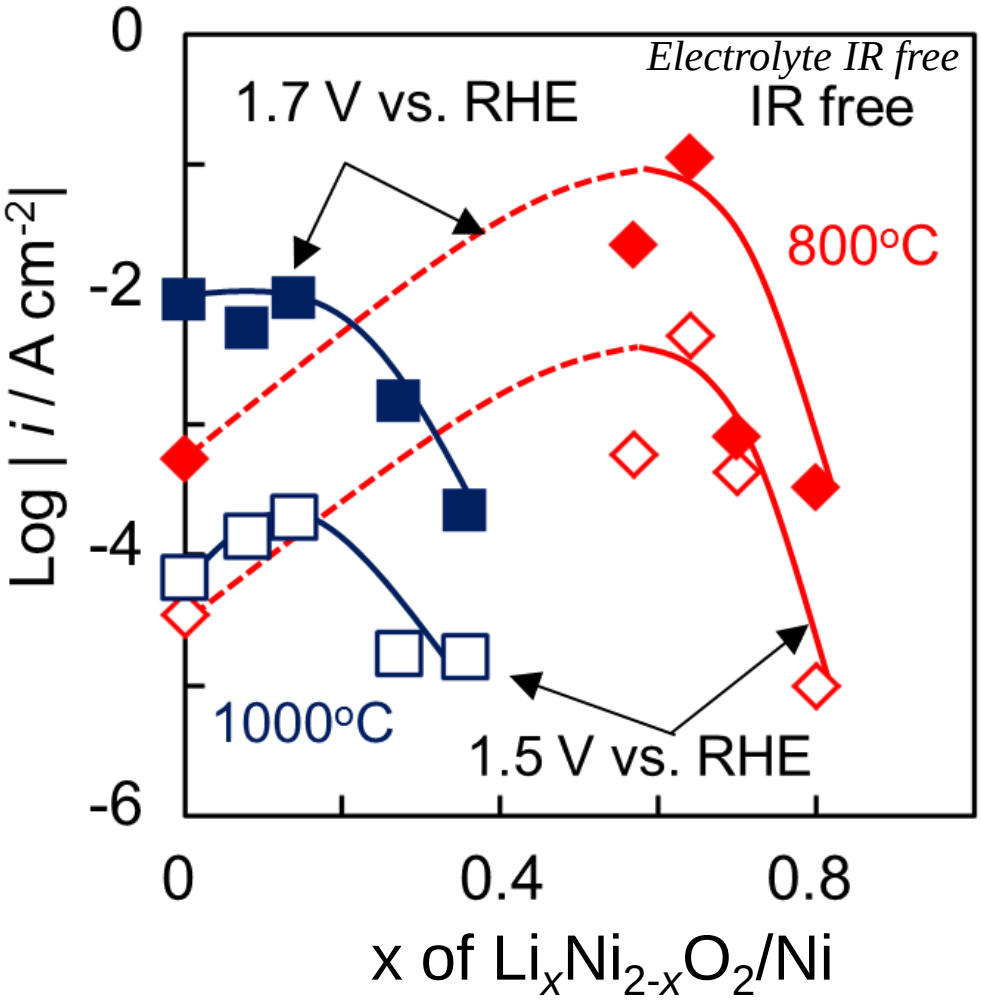

S. Fujita, I. Nagashima, Y. Sunada, Y. Nishiki, S. Mitsushima, Electrocatalysis. 8 (2017) 422–429.

24 Durability under 1.0 to 1.8 V of potential cycling

OER activity of the $Li_xNi_{2-x}O_2$/Nis was stable under potential cycling

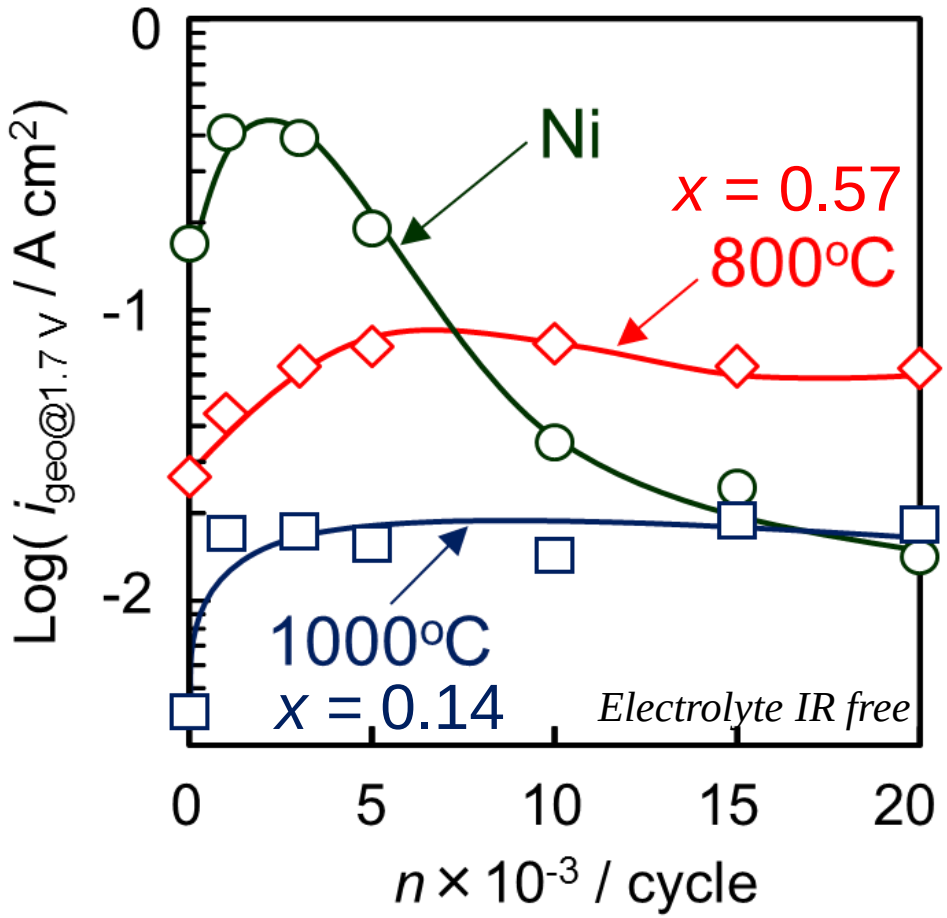

S. Fujita, I. Nagashima, Y. Sunada, Y. Nishiki, S. Mitsushima, Electrocatalysis. 8 (2017) 422–429.

25 EIS measurements of Ni and $Li_xNi_{2-x}O_2$/Nis

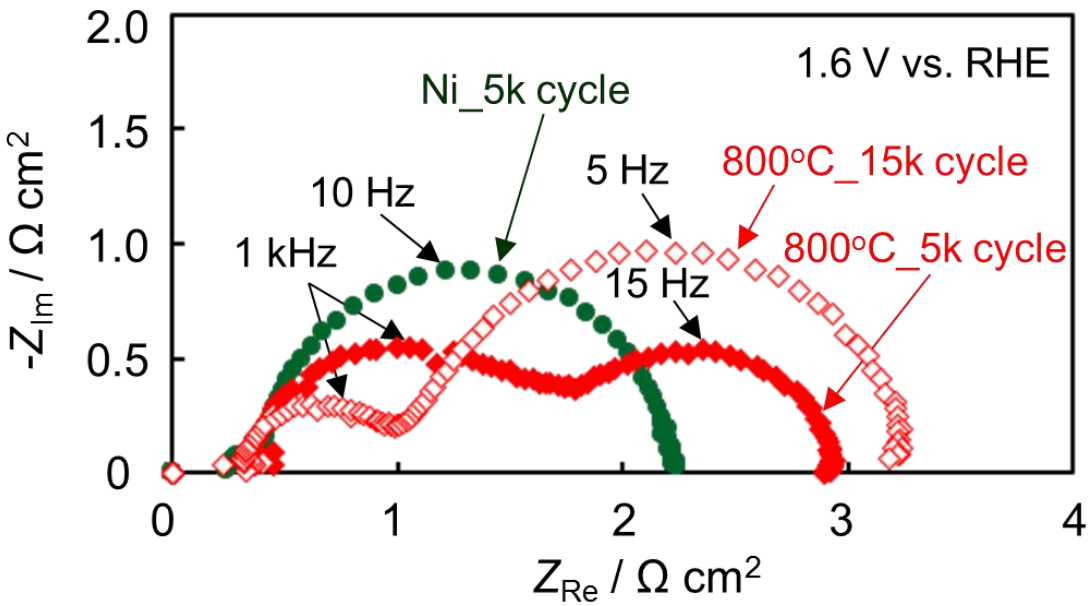

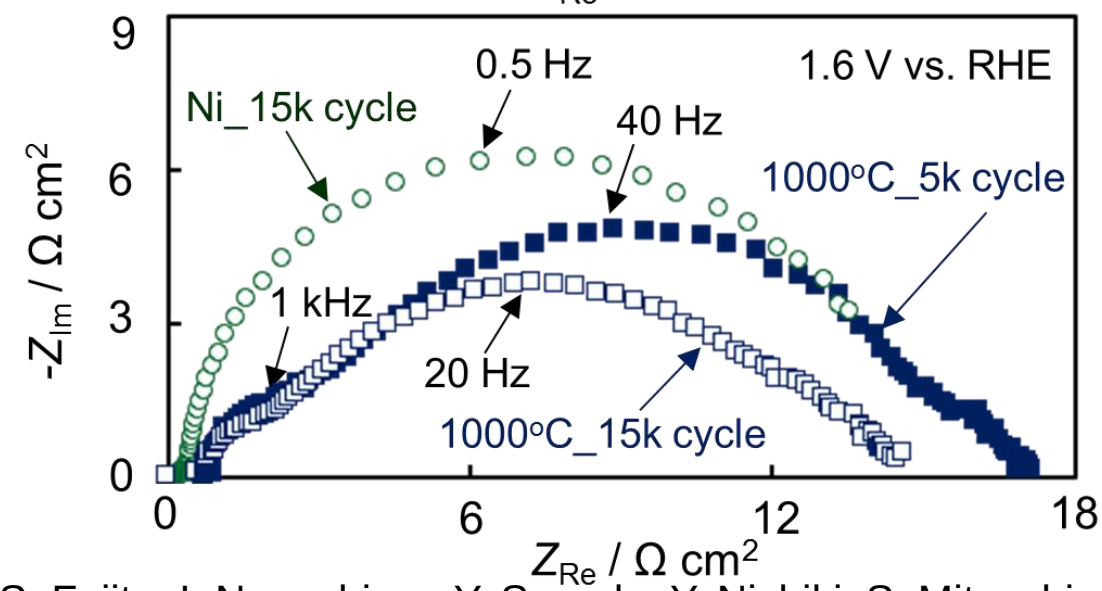

Ni: OER of low frequency arc increase with potential cycling

800°C: Relatively small OER and surface resistance of low and high frequency arcs were observed.

1000°C: Relatively large OER and surface resistance of low and high frequency arcs were observed.

S. Fujita, I. Nagashima, Y. Sunada, Y. Nishiki, S. Mitsushima, Electrocatalysis. 8 (2017) 422–429.

26 Tafel plot of the SSV at 5 mV s^{-1} on the Ni and $Li_xNi_{2-x}O_2$/Ni

- Activity of Ni decreased with potential cycling with simultaneously formation Ni(IV) around 1.55 V vs. RHE
- Activities of the $Li_xNi_{2-x}O_2$/Nis increased with potential cycling without Ni(IV) formation

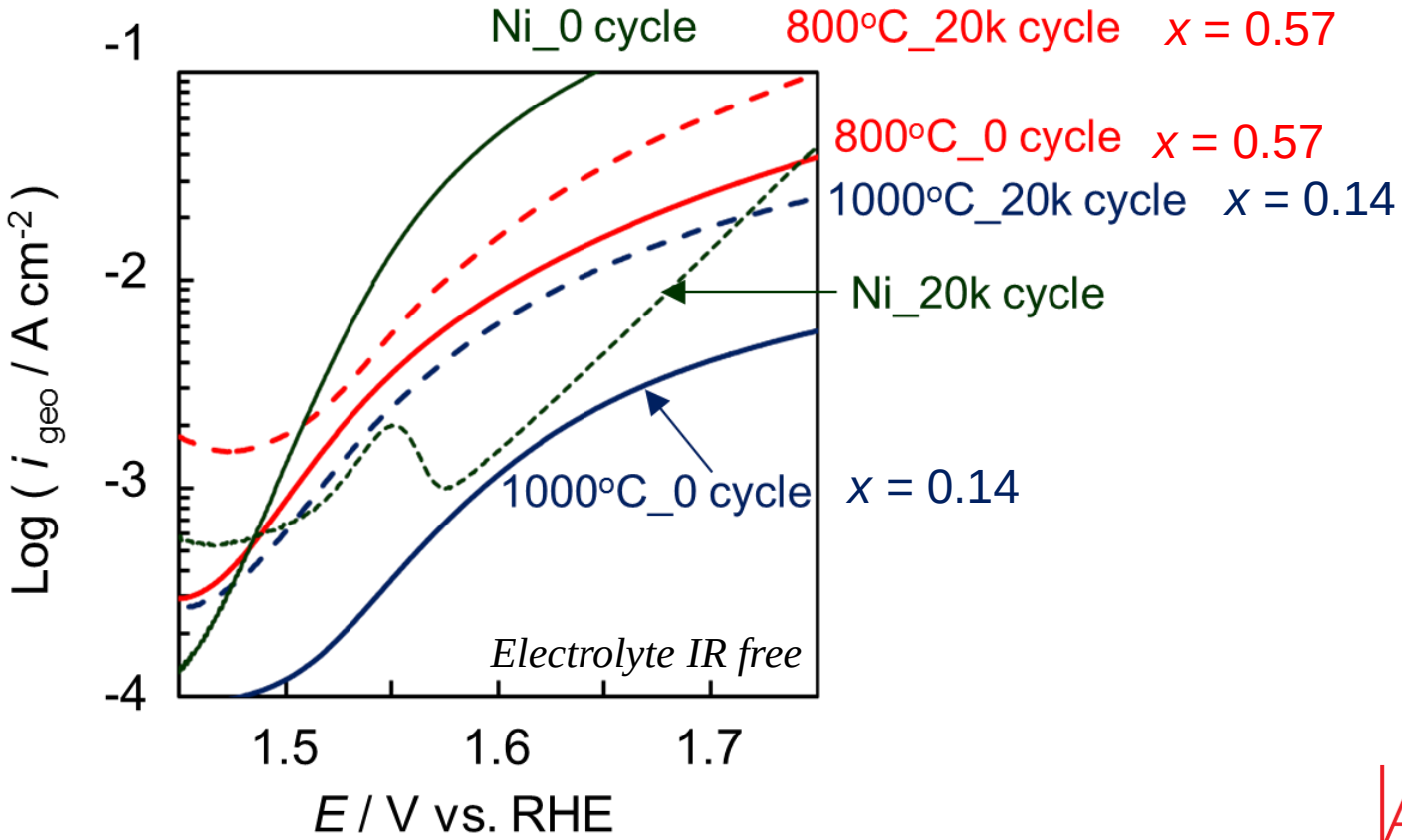

S. Fujita, I. Nagashima, Y. Sunada, Y. Nishiki, S. Mitsushima, Electrocatalysis. 8 (2017) 422–429.

27 CVs of before and after potential cycling

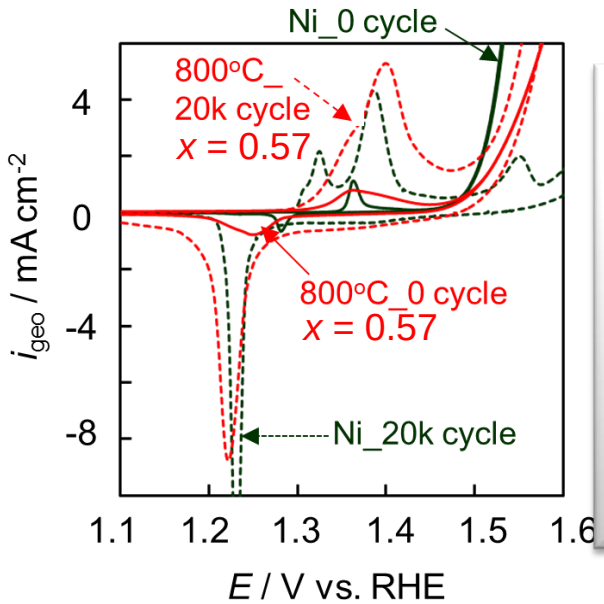

- Peaks of Ni(II)/Ni(III) for both Ni and $Li_xNi_{2-x}O_2$/Nis increased with potential cycling
- Peaks of Ni(II)/Ni(III) for 1000°C prepared was the most stable in these electrode.

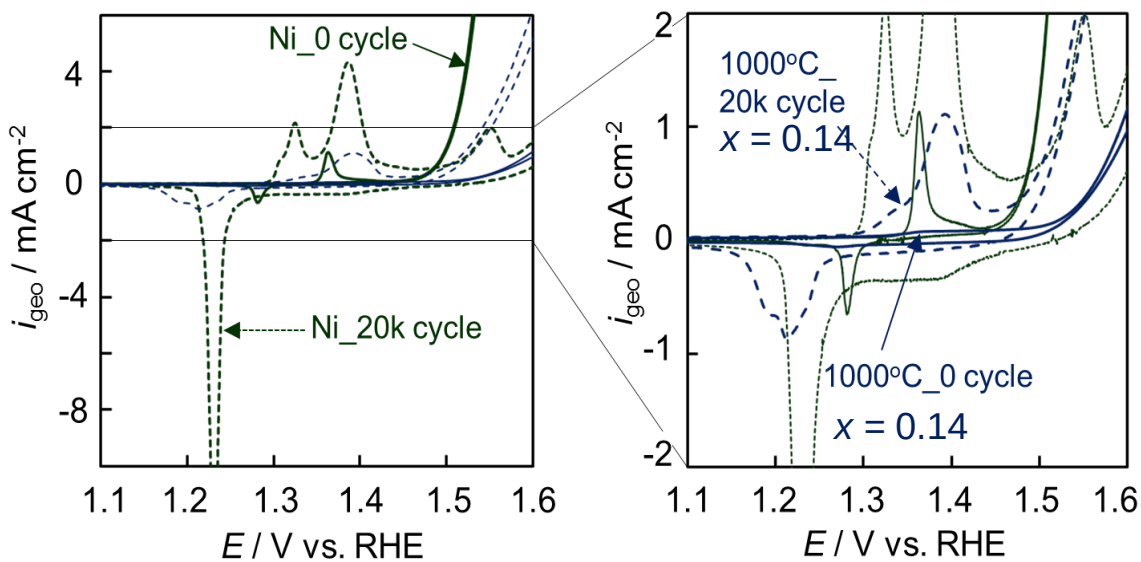

S. Fujita, I. Nagashima, Y. Sunada, Y. Nishiki, S. Mitsushima, Electrocatalysis. 8 (2017) 422–429.

28 Control of (Li)NiO layer by thermal decomposition

Advantage of $Li_xNi_{2-x}O_2$/Ni

- Improvement of the stability for specific activity without Ni(IV) formation

Disadvantage of $Li_xNi_{2-x}O_2$/Ni

- IR loss of electronic resistance of the (Li)NiO

Solution: Control of (Li)NiO layer to thinner and denser by thermal decomposition

- Low temperature preparation of 550°C for thermal decomposition and sintering
- Comparison of $LiNO_3$-$Ni(NO_3)_2$ and $LiNiO_3$-$Ni(COOH)_2$ precursor

S. Fujita, I. Nagashima, Y. Sunada, Y. Nishiki, S. Mitsushima, Electrocatalysis, 10.1007/s12678-017-0439-x

Thermal decomposed oxide film resistances

Surface oxide resistance of the acetate precursor electrode was the lowest in the $Li_xNi_{2-x}O_2$/Nis, and close to Ni because of the thin and dense with Li doped electroconductive layer

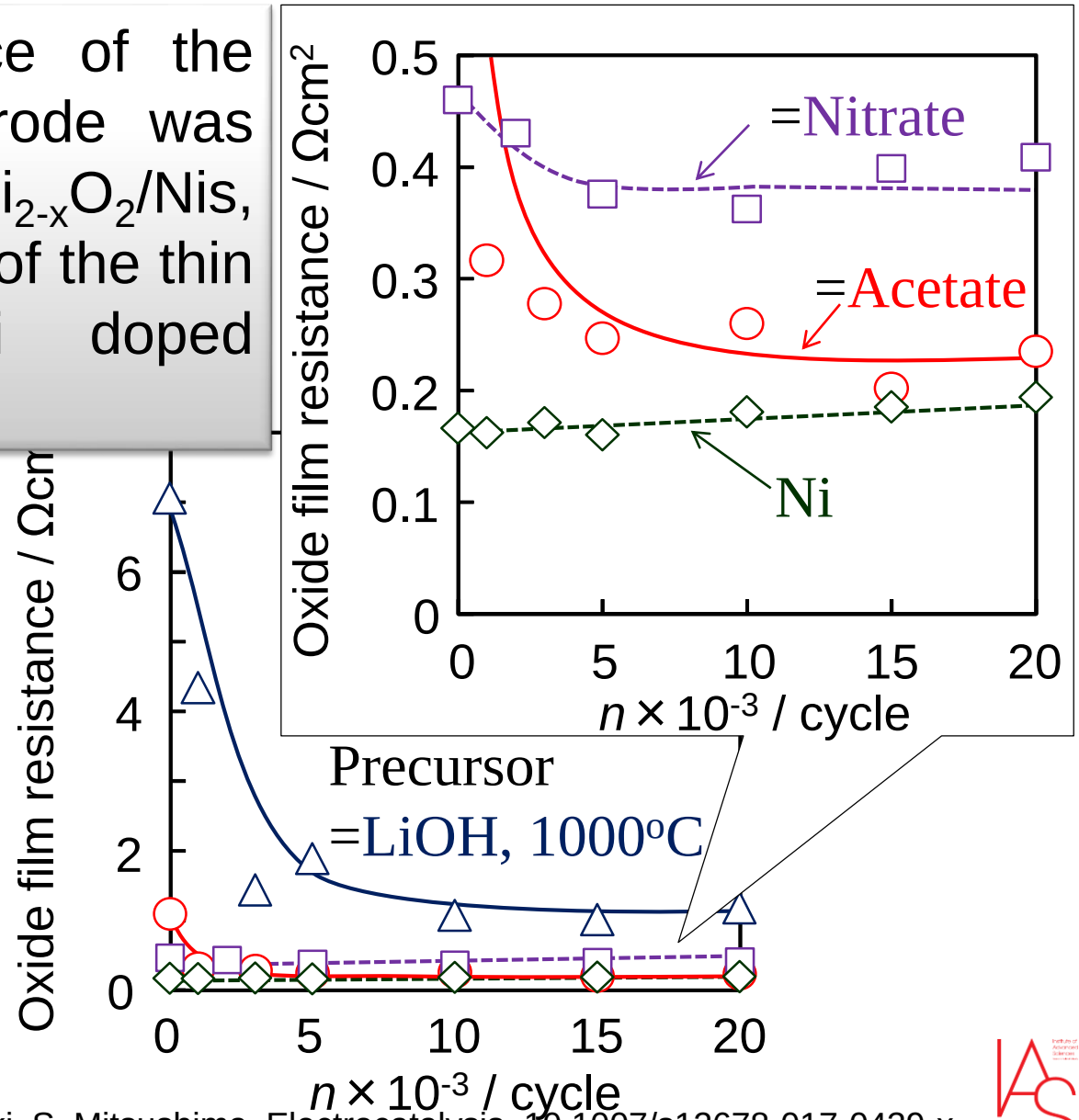

S. Fujita, I. Nagashima, Y. Sunada, Y. Nishiki, S. Mitsushima, Electrocatalysis, 10.1007/s12678-017-0439-x

30 SSVs at 5 mVs^{-1} of acetate and nitrate precursors

- Acetate precursor, which formed thin and dens layer, showed higher OER current and Tafel slope than the oxidation with LiOH
- Nitrate precursor, which formed porous layer, showed degradation like as Ni

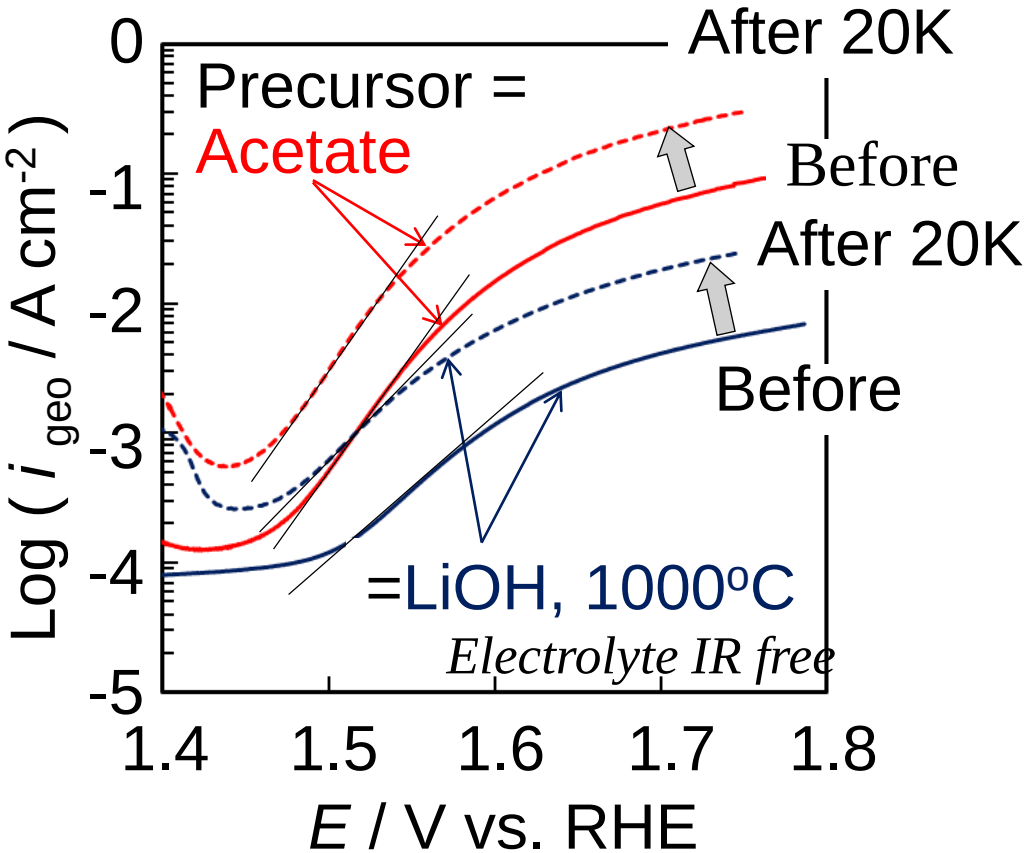

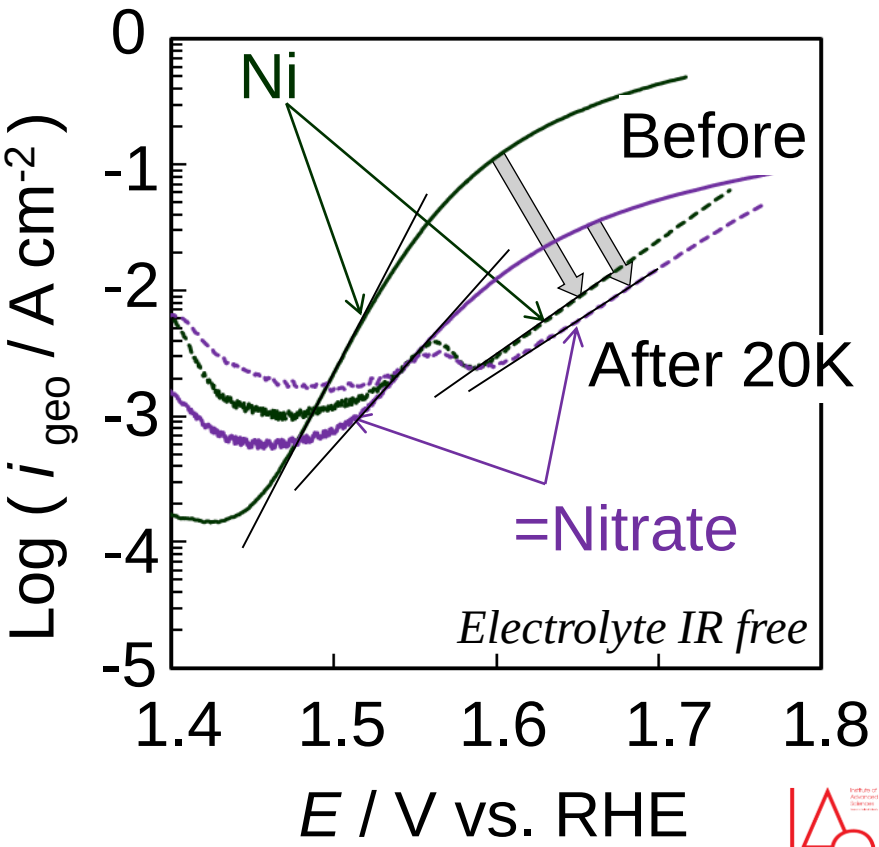

S. Fujita, I. Nagashima, Y. Sunada, Y. Nishiki, S. Mitsushima, Electrocatalysis, 10.1007/s12678-017-0439-x

31 Activity and stability for $Li_xNi_{2-x}O_2$/Ni of acetate precursor

Acetate precursor electrode showed the highest OER current in $Li_xNi_{2-x}O_2$/Nis, and the most stable in these electrodes

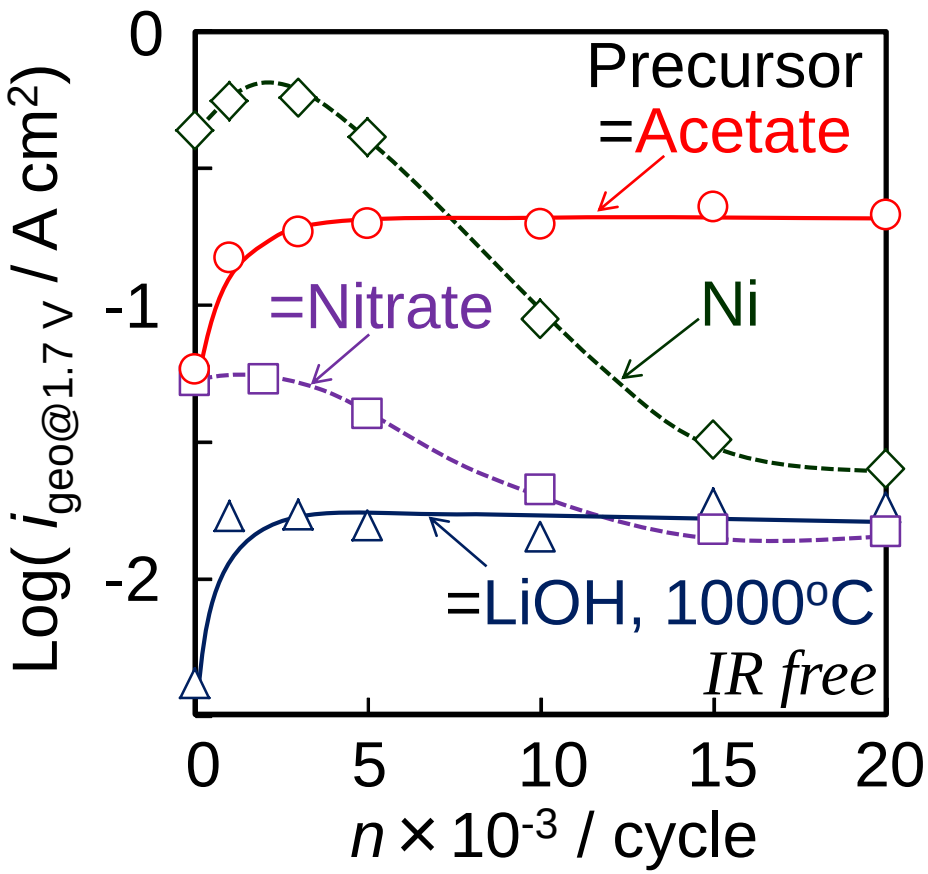

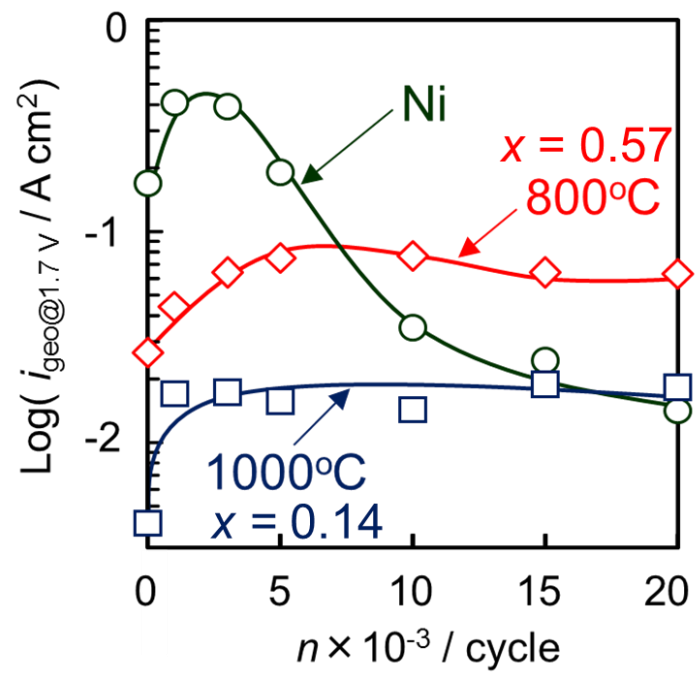

S. Fujita, I. Nagashima, Y. Sunada, Y. Nishiki, S. Mitsushima, Electrocatalysis, 10.1007/s12678-017-0439-x

Conclusion for $Li_xNi_{2-x}O_2$/Ni anodes

In order to develop anti-reverse current AWE anode, surface modification of Ni with Li doped oxide has been investigated

- Li doping increased electronic conductivity of the surface oxide with high valent Ni
- Appropriate Li doping increased OER activity of the surface oxide
- Excess Li doping decreased OER activity with the change of rate determining step
- Thin and dens (Li)NiO layer, which could be prepared with acetate precursor, showed the high activity and durability under potential cycling

Durable AWE with high performance would be developed with improvement of electrocatalysts

Contents

1. Introduction

2. Analysis of bipolar electrolyzer for alkaline water electrolysis

3. Active and durable anode for alkaline water electrolysis

4. Direct electrohydrogenation of toluene with water decomposition

5. Conclusion

34 Hydrogen energy carriers & secondary batteries

Energy density of energy carriers is as ten times as batteries (ca. 1/10 of fossil energies)

Energy carriers: Energetic materials for energy storage and transportation

	Pressurized hydrogen	Liquefied hydrogen	Liquefied ammonia	Toluene / Methylcyclohexane
Formula	H_2	H_2	NH_3	C_7H_8/C_7H_{14}
B. P. (°C)	-253	-253	-33.4	101
Density(g/cm^3)	0.0392(70MPa)	0.0706	0.682	0.769
H_2 ΔG density (Wh/kg)	32,900	32,900	5,810	2,010
(Wh/L)	1,290(70MPa)	2,330	3,960	1,550

Secondary batteries: Energy storage systems

	Redox flow	Na-S	Lead acid	Lithium ion	Ni-MH	Zn-Br
Active material (+)/(-)	VO^{2+} / V^{2+}	S / Na	PbO_2 / Pb	$LiMO_2$ / LiC_6	NiOOH / MH	Br_2 / Zn
energy density Theoretical	100	786	167	392 - 585	225	428
Actual (Wh/kg)		110	35	120	60	

35 Hydrogenation using renewable energies

Electrohydrogenation of toluene has the most highest theoretical energy conversion efficiency for energy carrier synthesis

88%（=1.08/1.23）of hydrogen production of water electrolysis

Renewable energies

Direct electrohydrogenation →

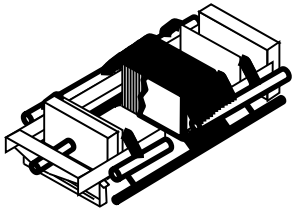

U^o = **1.08 V**

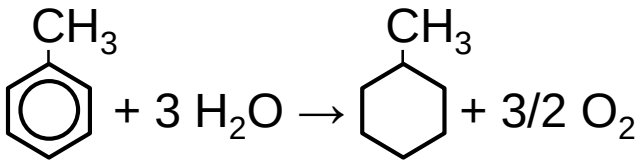

Water electrolysis → (storage) → hydrogenation →

$3\ H_2O \rightarrow 3H_2 + 3/2\ O_2$

U^o = **1.23 V**

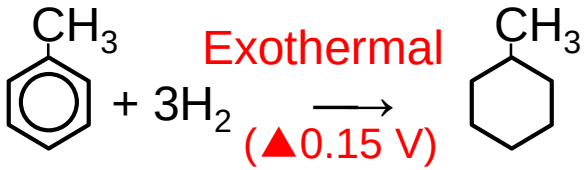

S. Mitsushima, Y. Takakuwa, K. Nagasawa, Y. Sawaguchi, Y. Kohno, K. Matsuzawa, Z. Awaludin, A. Kato, Y. Nishiki, Electrocatalysis. 7 (2016) 238–131.

Direct electrohydrogenation electrolysis

A new efficient energy carrier synthesis process

Combination of electrohydrogenation and water decomposition

Cathode: 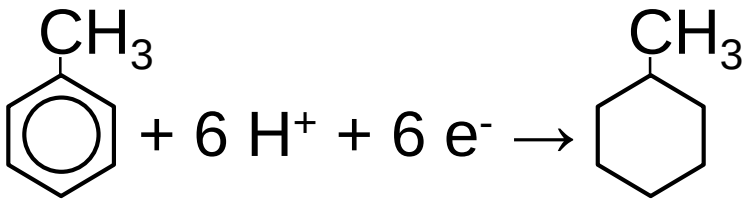

$+ 6\ H^+ + 6\ e^- \rightarrow$ $E^o = 0.15$ V vs. SHE

Anode: $3\ H_2O \rightarrow 6H^+ + 3/2\ O_2 + 6e^-$ $E^o = 1.23$ V vs. SHE

Overall: 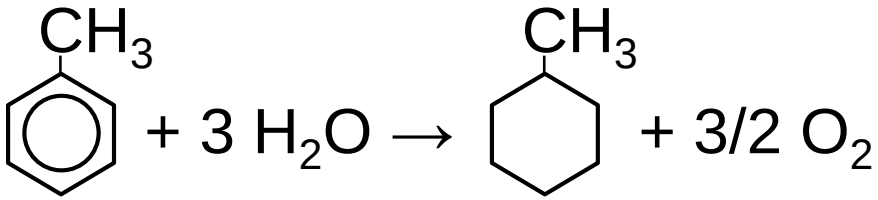

$+ 3\ H_2O \rightarrow$ $+ 3/2\ O_2$ $U^o = 1.08$ V

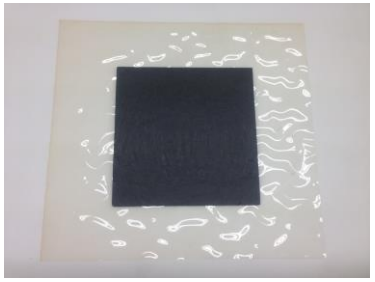

Cathode membrane assembly: PtRu/C catalyst layer on Nafion 117

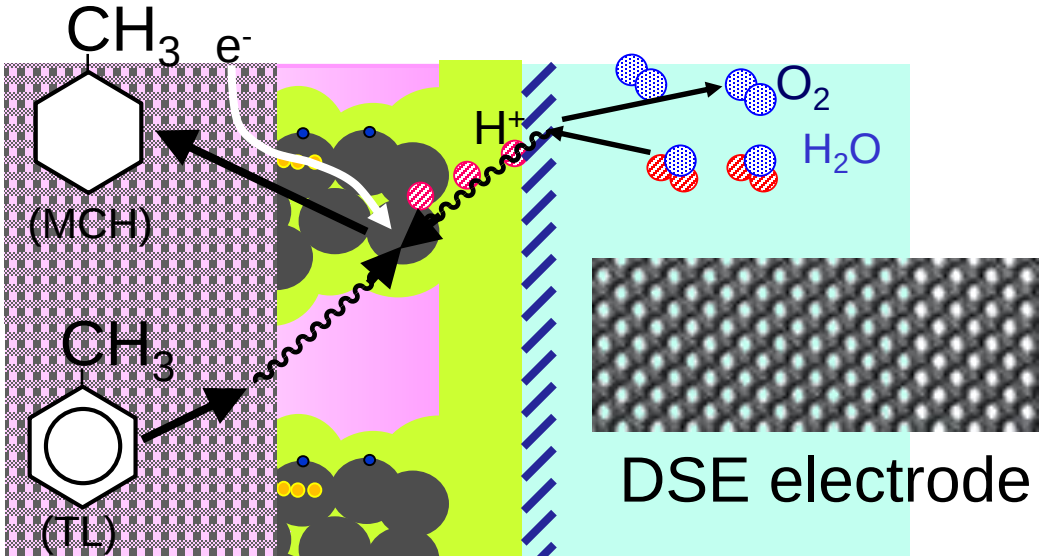

37 Polarization curves for Pt/C and PtRu/C

- Onset potential of reduction was positive
- Gas evolution was not observed
- MCH was an only product
- PtRu/C had larger reduction current than Pt/C

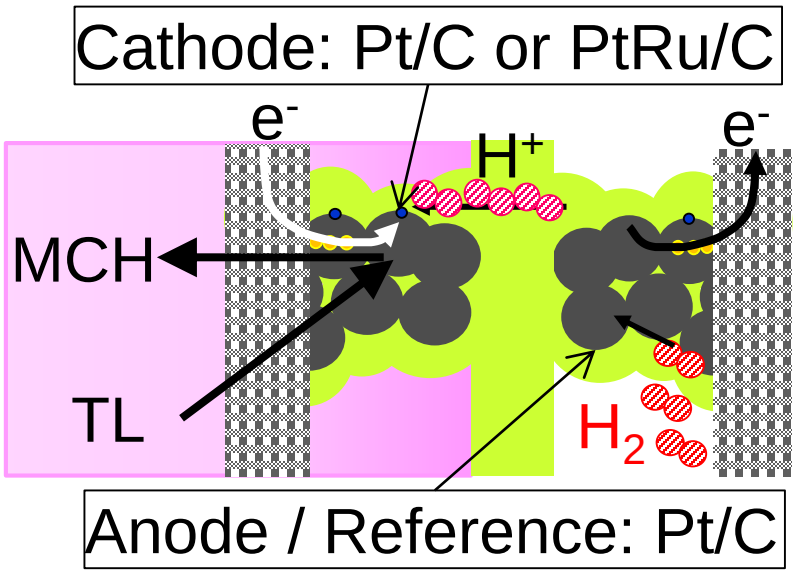

Fig. Configuration of a membrane half cell .

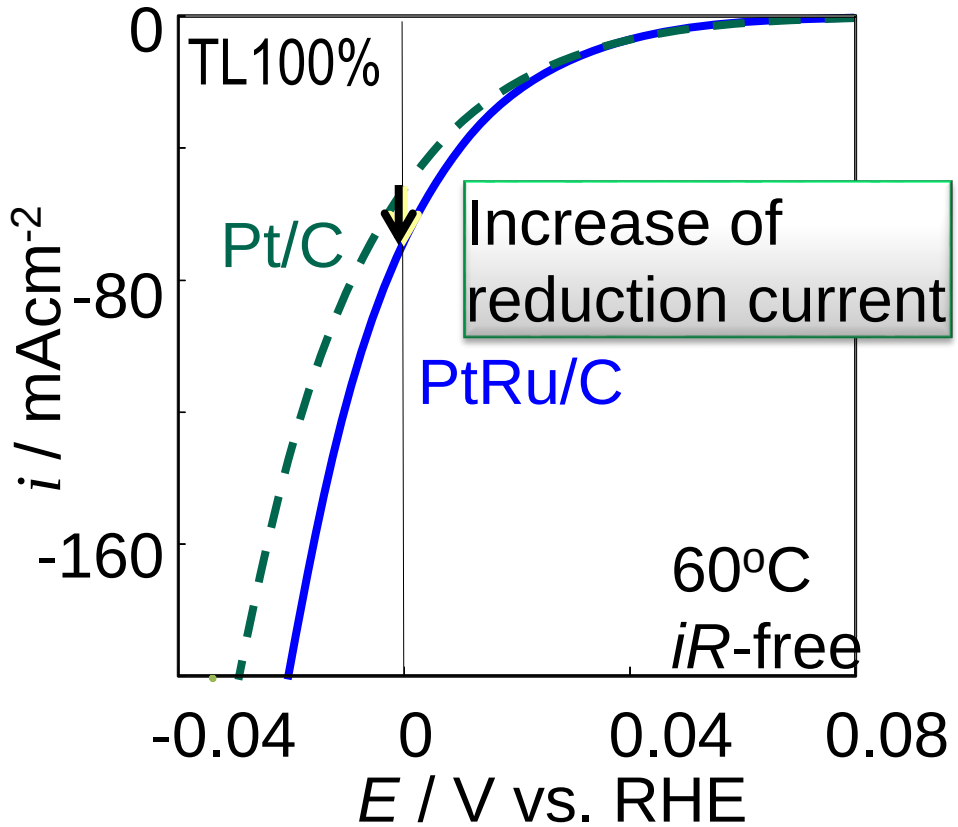

S. Mitsushima, Y. Takakuwa, K. Nagasawa, Y. Sawaguchi, Y. Kohno, K. Matsuzawa, Z. Awaludin, A. Kato, Y. Nishiki, Electrocatalysis. 7 (2016) 238–131.

38 Hydrogenation current as a function of temperature

- PtRu/C had larger reduction current than Pt/C below 70°C
- PtRu/C had the maximum currents at 60 °C, while Pt/C increased with temperature / This might be affected by the adsorption of TL and MCH

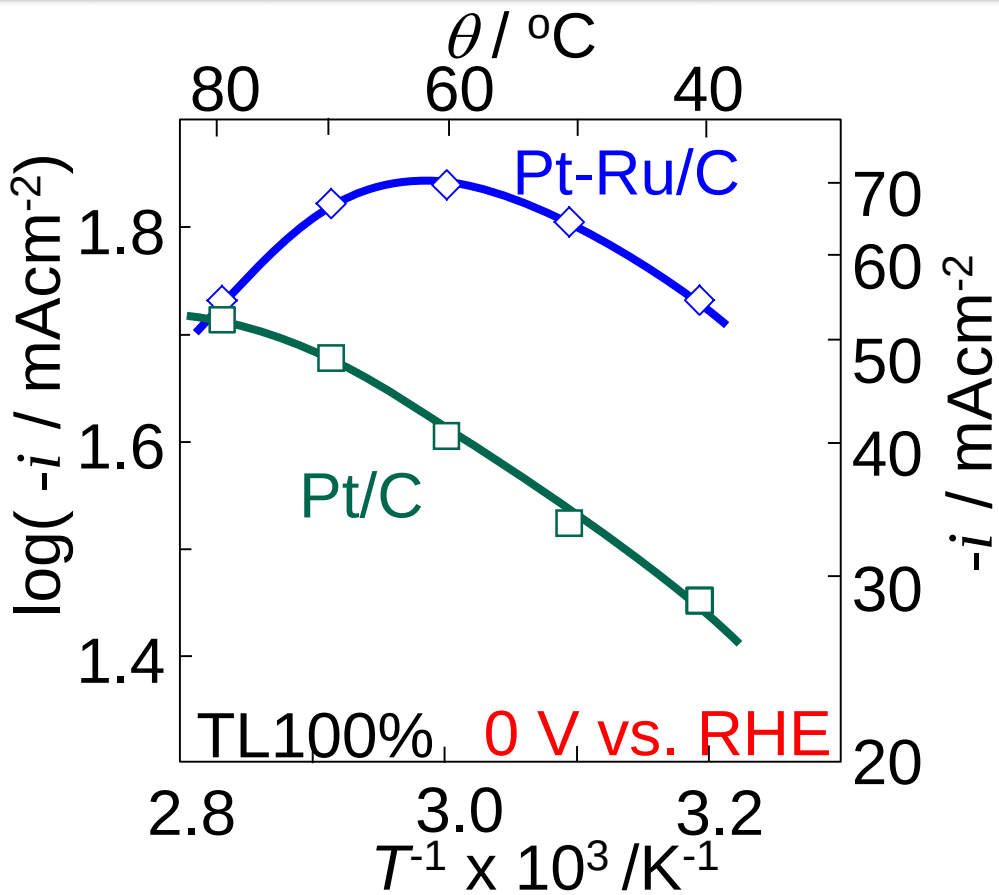

S. Mitsushima, Y. Takakuwa, K. Nagasawa, Y. Sawaguchi, Y. Kohno, K. Matsuzawa, Z. Awaludin, A. Kato, Y. Nishiki, Electrocatalysis. 7 (2016) 238–131.

39 Anode for oxygen evolution reaction

- TL inhibited OER and accelerated degradation for IrO_2/Ti
- TL inhabitation was suppressed for IrO_2-Ta_2O_5/Ti and IrO_2-Ta_2O_5-ZrO_2/Ti
- Activity improved not only increase of effective surface area by Ta and ZrO_2 addition

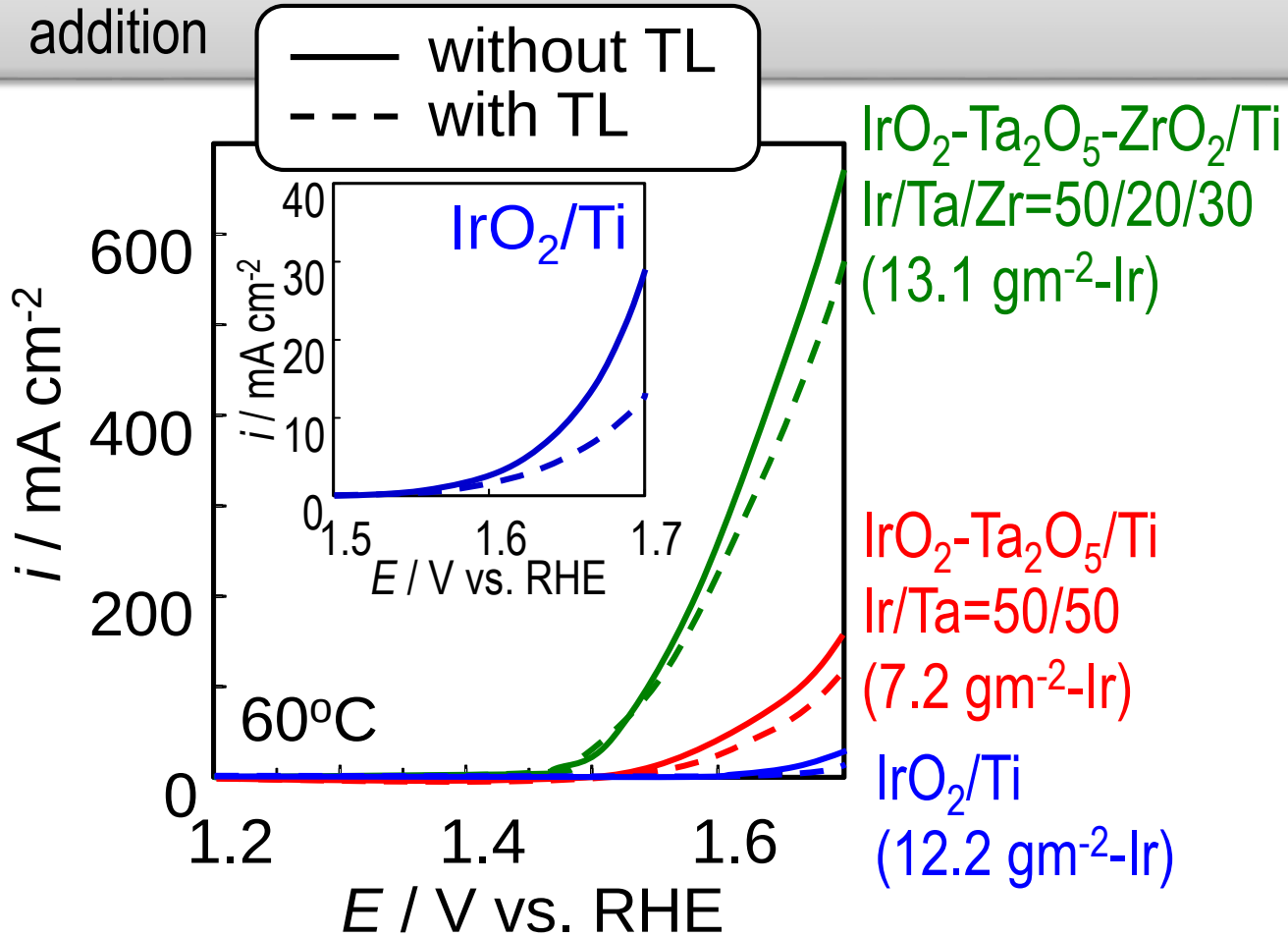

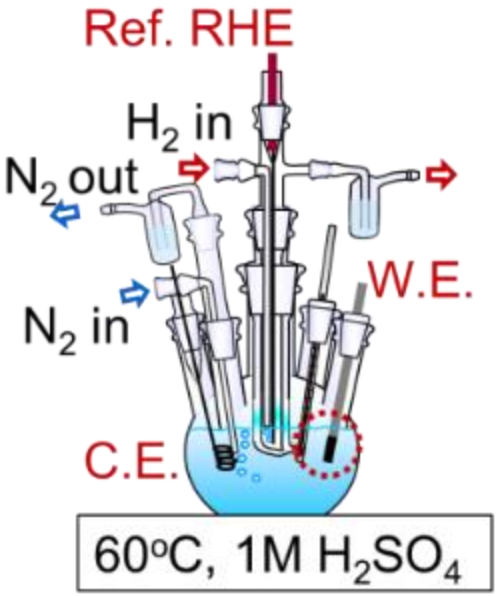

Nagai, K. Nagasawa, and S. Mitsushima, *Electrocatalysis*, **7**, 441–444 (2016)

40 Flow field design for cathode

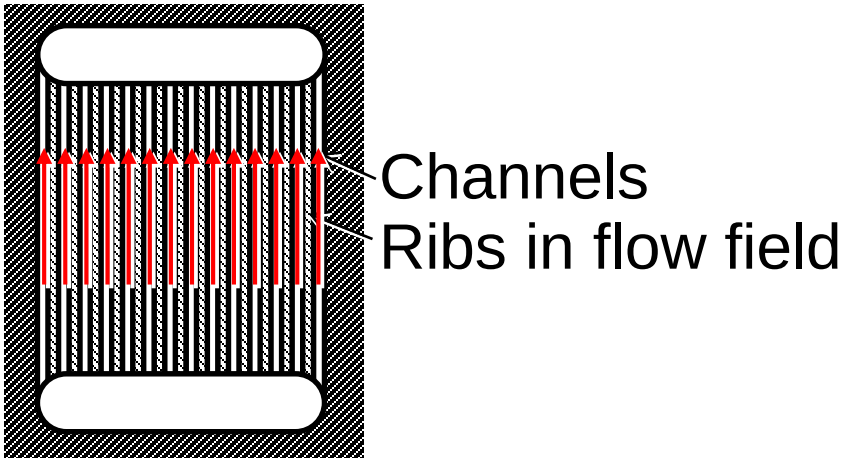

a) Parallel flow channel

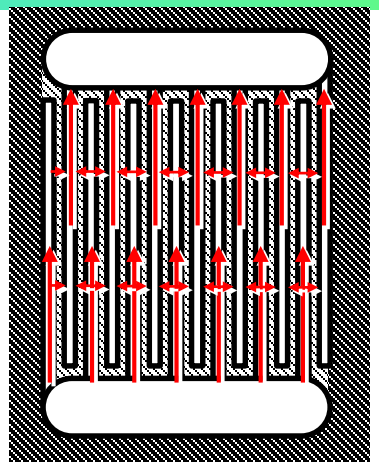

c) Interdigitated flow channel

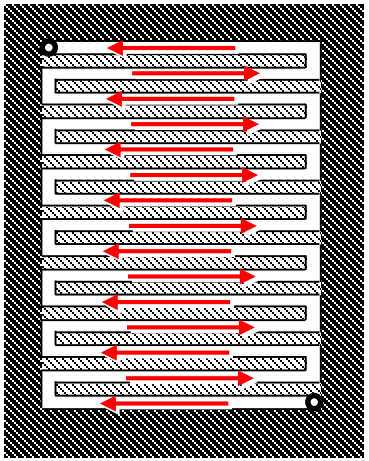

b) Serpentine flow channel

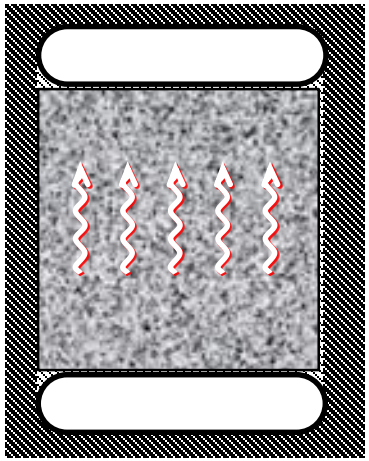

c) Porous carbon flow field

K. Nagasawa, A. Kato, Y. Nishiki, Y. Matsumura, M. Atobe, S. Mitsushima, Electrochim. Acta. 246 (2017) 459–465.

41 LSV curves for various flow fields

- The cell voltages: Porous < Parallel < Interdigit < Serpentine
- Activation overpotentials were almost same for all flow fields
- 0.18 ~ 0.25 Ωcm^2 of internal resistance could not explain the difference of the cell voltages
- EIS showed cathodic mass transfer resistance affected to the cell voltages

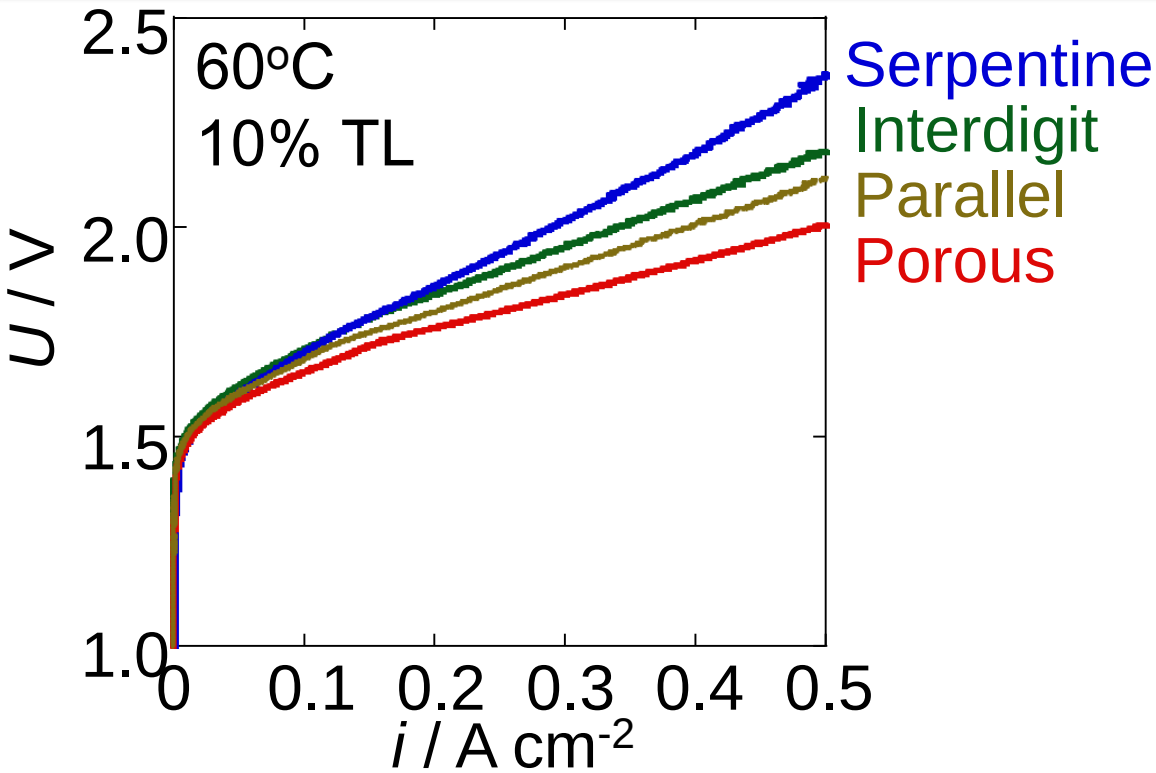

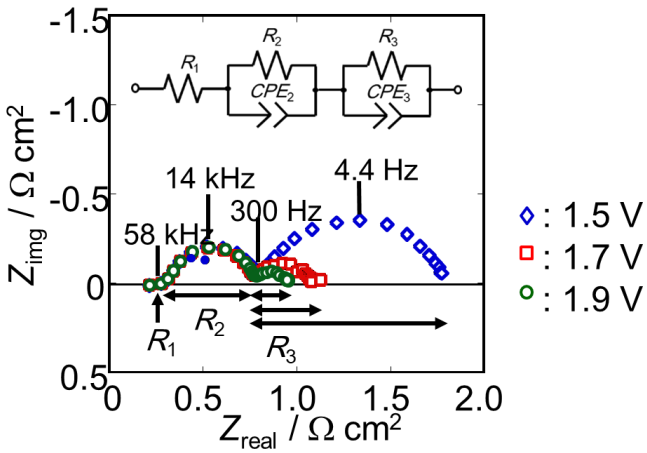

K. Nagasawa, A. Kato, Y. Nishiki, Y. Matsumura, M. Atobe, S. Mitsushima, Electrochim. Acta. 246 (2017) 459–465.

42 Current efficiency as function of current for 10% TL

- Porous flow field showed 100% of current efficiency up to 0.15 Acm^{-2}
- Parallel was better than serpentine and interdigit a little
- This turn is as same as cathodic reaction resistance

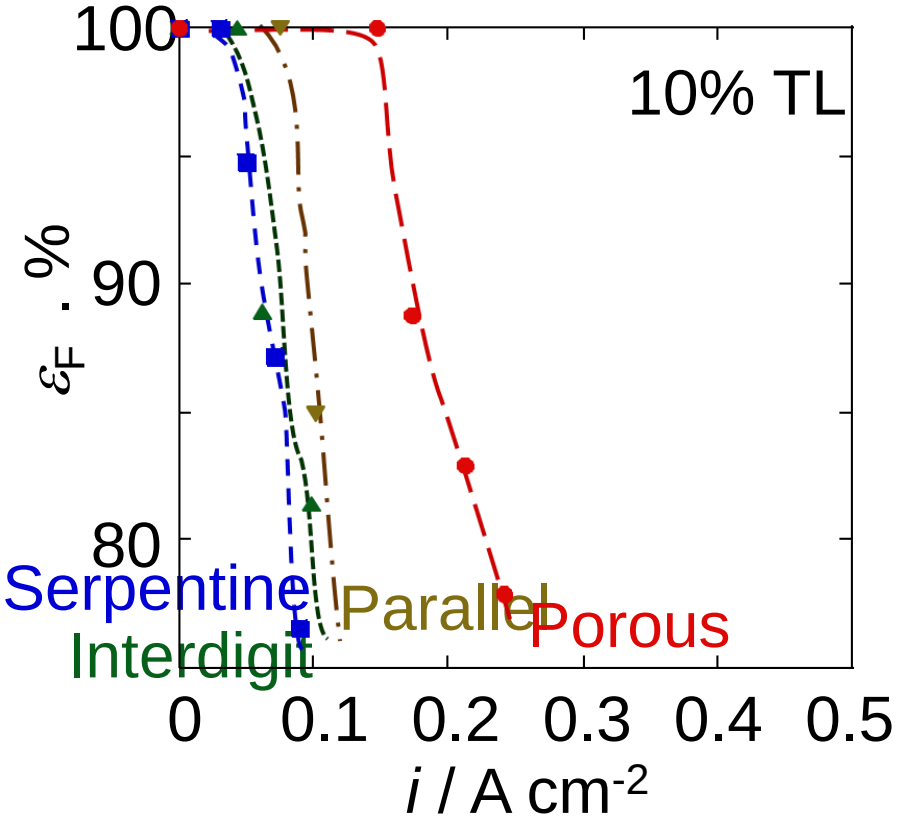

$$\varepsilon = \frac{hydrogenation}{applied} = \frac{applied - H_2\ evolution}{applied}$$

K. Nagasawa, A. Kato, Y. Nishiki, Y. Matsumura, M. Atobe, S. Mitsushima, Electrochim. Acta. 246 (2017) 459–465.

43 Decrease of H_2 bubble residence with flow field catalyst

- H_2 bubble reacts with TL on Pt catalyst
- Interruption of TL transfer by H_2 bubble is suppressed

→ **Cathode reaction resistance decreases with hydrogenation catalyst on flow field**

Decrease of local TL concentration

Cathode catalyst layer

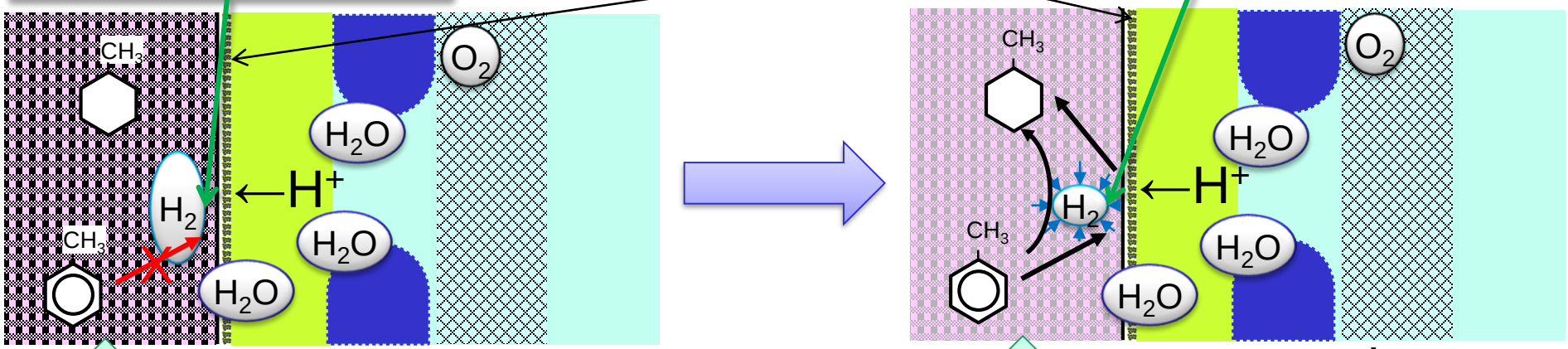

Porous carbon flow field without Pt catalyst

Pt catalyst loaded porous carbon flow field

S. Mitsushima, K. Nagasawa, A. Kato, Y. Nishiki, 232nd ECS Meeting (2017) #1673

44 Improvement of current distribution with anode structure

Fine mesh anode makes uniform current flow lines in thin electrolyte membrane to decrease apparent reaction resistance caused by charge and mass transfer

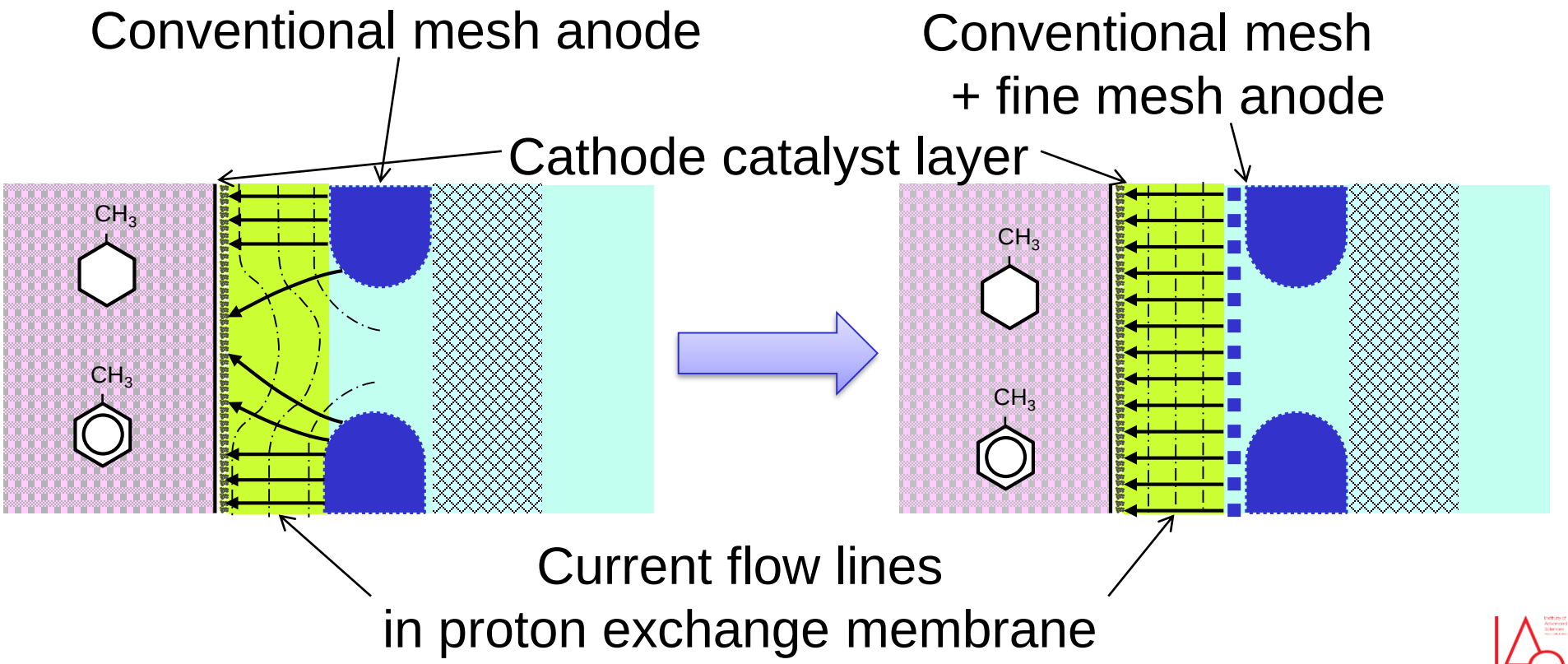

S. Mitsushima, K. Nagasawa, A. Kato, Y. Nishiki, 232nd ECS Meeting (2017) #1673

45 Cell voltage reduction

Cell voltage reduced with the improvement of flow field and anode structure

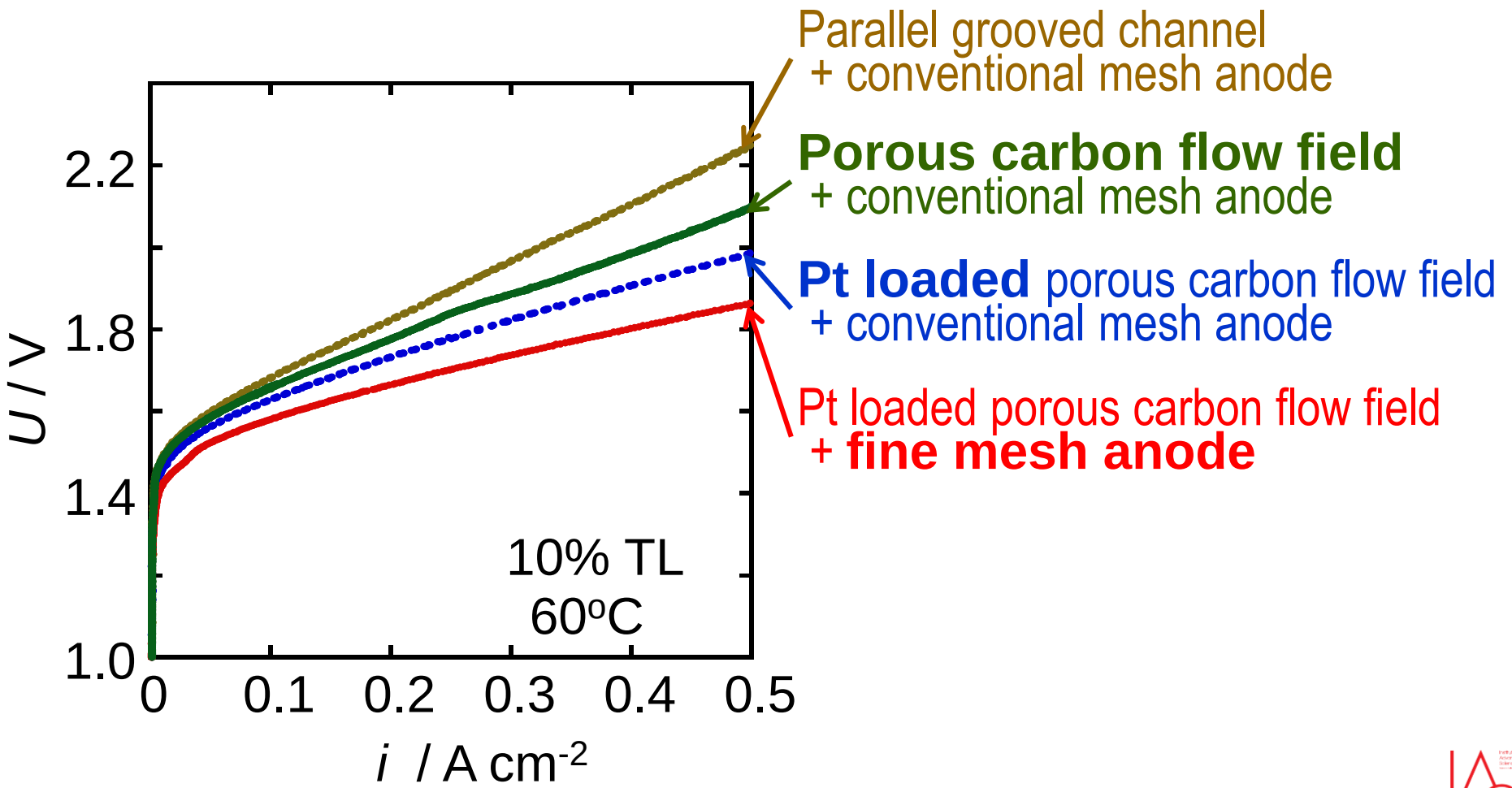

S. Mitsushima, K. Nagasawa, A. Kato, Y. Nishiki, 232nd ECS Meeting (2017) #1673

46 Enhancement of current efficiency

Current efficiency increased with the improvement of flow field and anode structure

$$\varepsilon_F = \frac{hydrogenation}{applied} = \frac{applied - H_2\ evolution}{applied}$$

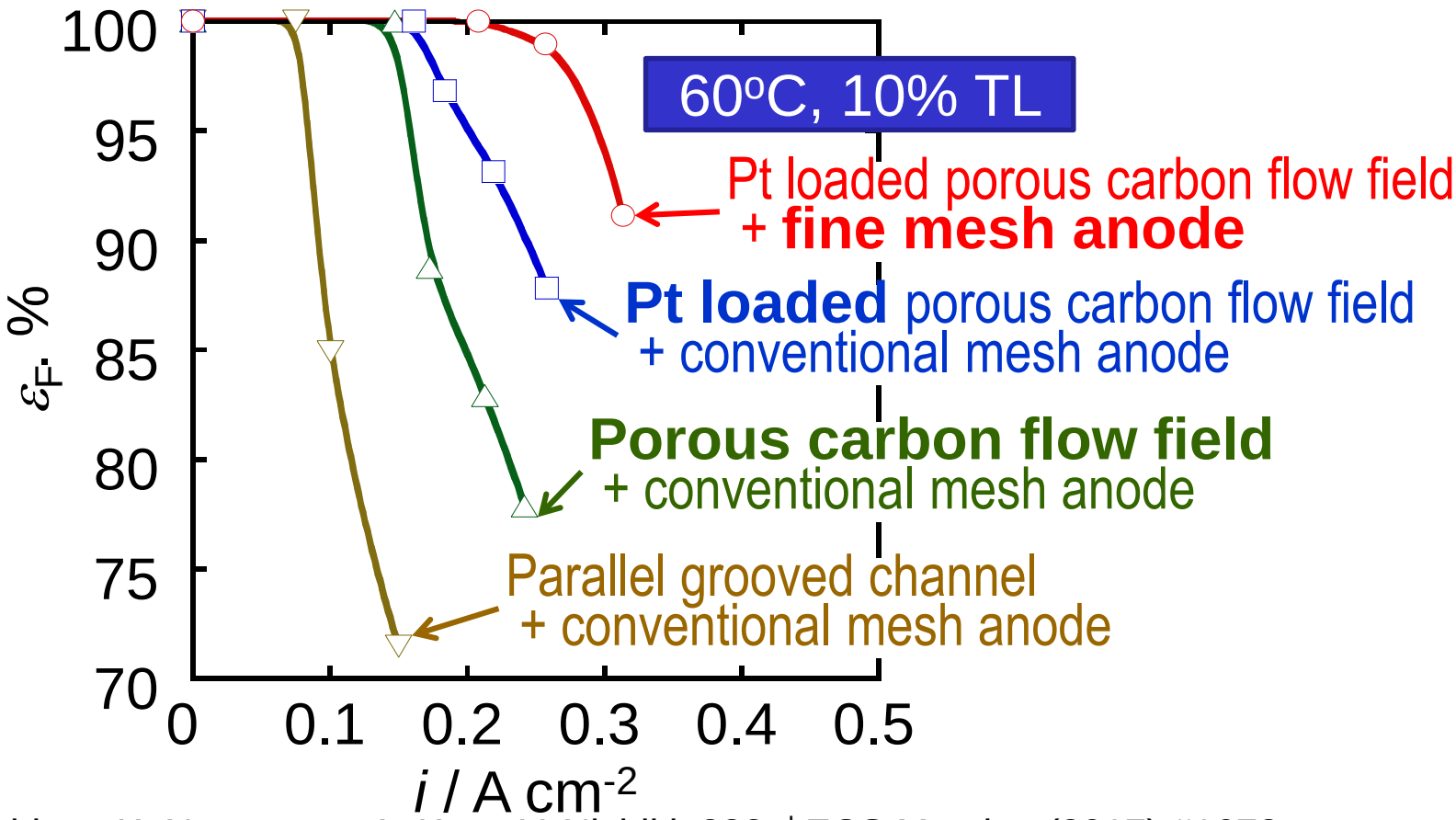

S. Mitsushima, K. Nagasawa, A. Kato, Y. Nishiki, 232nd ECS Meeting (2017) #1673

47 Conversion under one through operation

- Cell voltage was almost independent from flow rate of TL
- Conversion was almost as same as theoretical value, and 1.7 V @ 0.4 A cm^{-2} with more than 90% conversion and 95% current efficiency

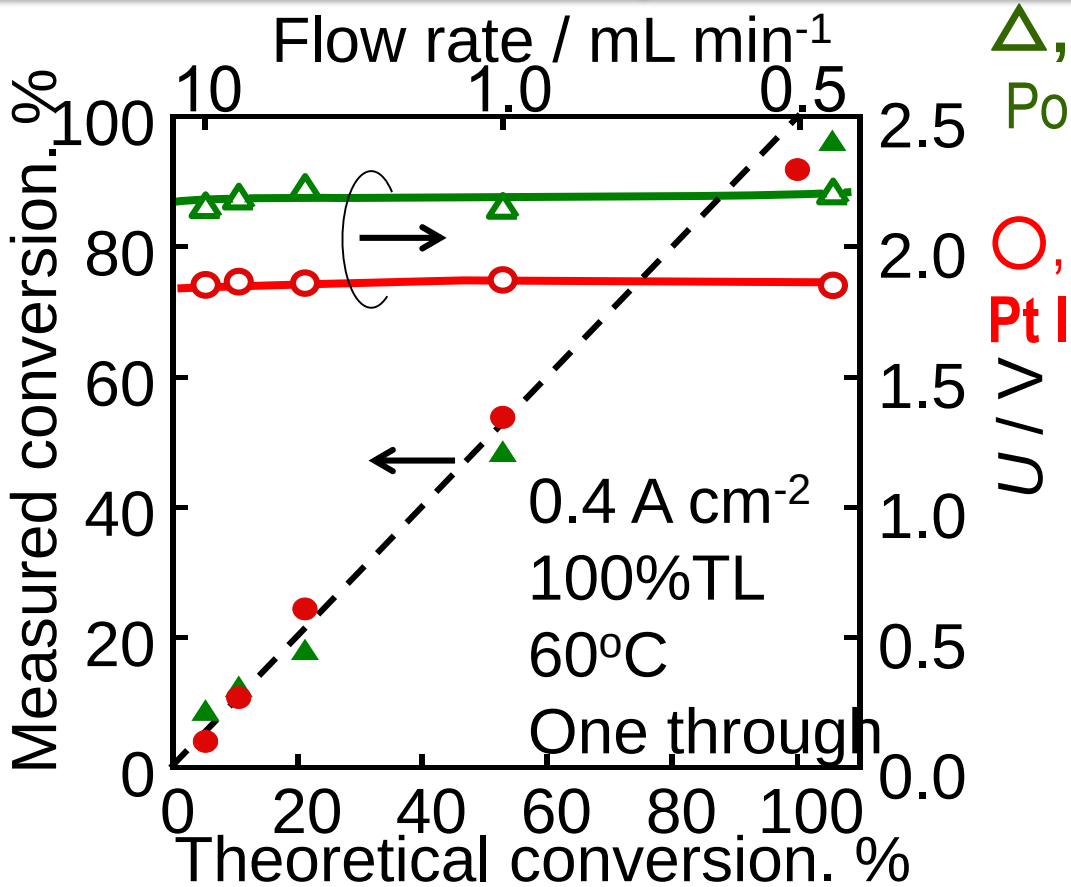

△, ▲:
Porous carbon flow field
+ conventional mesh anode

○, ●:
Pt loaded porous carbon flow field
+ fine mesh anode

S. Mitsushima, K. Nagasawa, A. Kato, Y. Nishiki, 232nd ECS Meeting (2017) #1673

48 Conclusion for direct energy carrier synthesis

As a high energy conversion efficiency for energy carrier synthesis process, membrane electrolysis for toluene hydrogenation with water decomposition is proposed

Present performance is 1.7 V of cell voltage at 0.4 A cm^{-2} with more than 90% conversion and 95% current efficiency

<Important technologies>

- PtRu/C and Nafion 117 cathode membrane assembly
- Platinized porous flow field
- Zero-gap fining of anode

Conclusion

- Hydrogen is an energy carrier for artificial hydrogen redox system to decrease carbon dioxide emission
- Electrolysis is the most realistic technology to produce chemical energy using renewable electricity with development for fluctuated power supply
- Alkaline water electrolysis is less expensive hydrogen production process and will be able to improve durability under potential cycling to connect renewable energies
- Direct electrohydrogenation of toluene with water decomposition, which is very efficient energy career synthesis process with renewable energies

50 Acknowledgment

These works were supported and/or cooperated by following funding agencies, universities, and industrial partners. The Institute of Advanced Sciences (IAS) in YNU is supported by the MEXT Program for Promoting the Reform of National Universities. I appreciate person concerned.